Goldeneye AB1

Raghav Anand, Alec English, Dante Gao,
Saunon Malekshahi, Rohan Sinha, Noah Stevenson

Faculty Advisor: Professor Stuart Bale, Ph.D.
Director of Space Sciences Laboratory

University of California, Berkeley

NASA Advanced Air Vehicles Design Competition
Supersonic Division

June 12, 2017

Team Members

First-Year Undergraduates

Raghav Anand: Electrical Engineering and Computer Science

Second-Year Undergraduates

Alec English: Physics and Mechanical Engineering

Dante Gao: Mechanical Engineering

Saunon Malekshahi: Mechanical Engineering

Rohan Sinha: Mechanical Engineering and Electrical Engineering and Computer Science

Noah Stevenson: Physics

To whom it may concern,

As the faculty advisor for UC Berkeley's Goldeneye AB1 design team, I affirm the following:

1. All work and writing herein was completed by the students alone, at all stages of the design process, without any professional assistance, and is either original or properly cited, not plagiarized.

2. The students received no NASA funds at any point during the project.

3. I have direct NASA funding of $1,067,947. I am also NASA Principal Investigator on an instrument suite for the Solar Probe Plus mission (Parker Solar Probe), which is funded as a $60 million subcontract from the Applied Physics Laboratory at Johns Hopkins.

Signed,

Stuart D. Bale
Director of Space Sciences Laboratory
Professor of Physics
University of California, Berkeley

Abstract

In October of 2003, the Concorde was retired from service, signaling the end of an era. The airliner was one of only two passenger planes to ever fly supersonic, dominating this market for a quarter-century. Since the Concorde's final flight, commercial aviation has been confined to subsonic aircraft, marking the first time in history that this industry has regressed technologically. With little incentive, aerospace companies have spent the last decade and a half tweaking and refining the designs of existing aircraft rather than innovating bold new ideas.

However, we are on the cusp of a new chapter in the ongoing history of supersonic flight. In the spirit of inquiry, discovery, and entrepreneurship, we are pleased to present Goldeneye AB1, a supersonic business jet concept that is the first of its kind. A joint venture between the College of Engineering and Space Sciences Laboratory, Goldeneye is the first supersonic commercial plane to feature a variable-geometry wing. With its stowed radial wing extension panel, Sears-Haack fuselage, and adjustable engine intake design, the AB1 significantly reduces noise and drastically improves aerodynamic efficiency in comparison to other supersonic aircraft. While unconventional by design, Goldeneye AB1 presents advancements that are unprecedented in the world of supersonic aviation, rendering it capable of changing the industry forever.

Goldeneye's target cruise speed is Mach 1.7, though it can reliably cruise anywhere from Mach 1.6-1.8. The AB1 attains a total specific fuel consumption (TSPC) of 0.93, with its engines providing 4833.29 lbf (21722 N) of thrust. Goldeneye can traverse its maximum range of 4227 nautical miles in just 3.96 hours, consuming 17853 lb of fuel in the process. Designed to carry up to 12 passengers, the AB1 achieves 2.84 passenger-miles per pound of fuel, making it one of the most efficient supersonic passengers planes ever introduced. Slated to enter the market by 2025, Goldeneye's sleek, versatile, and economical design will make it the premier contender in the near future of commercial supersonic aviation.

1 Introduction

The most prominent supersonic plane to ever fly was the Concorde, a passenger jet airliner jointly developed by Aérospatiale and the British Aircraft Corporation (BAC). During its 27-year service history, the Concorde became a symbol of innovation and technological prowess. It set countless airspeed and flight duration records, and logged more supersonic flight hours than all other aircraft combined. Despite its impressive track record, the Concorde was eventually forced out of service due to a combination of declining passenger numbers, increasing maintenance and operational costs, and the notorious Air France Flight 4590 incident of 2000. In short, the plane became a financial liability for Air France and British Airways to fly, which ultimately led to its retirement. But the "Great White" was more than a decommissioned airliner; it was a spectacle to behold. Its sleek ogival delta wing and tailless design set it apart from all other aircraft in its class. The Concorde made its mark in history by fully embracing the most futuristic visions of commercial travel, inspiring a generation of aviation enthusiasts.

In recent years, aerospace companies have begun to reconsider the allure of supersonic flight. At the forefront of this movement is Boom Technology, a startup whose mission is to design a supersonic civilian jet with the eventual goal of introducing it into the commercial aviation market. Decades of advanced military research surrounding topics from variable geometry wings to unconventional engine designs is now being undertaken again for the first time in over a decade. Though it is still early, the current technological and economical climate may soon give way to a future where supersonic flight can once again be a thriving industry.

Our vision in developing a supersonic business jet concept is to combine the spirit of innovation demonstrated by the Concorde with careful consideration of the modern need for environmental and economical sustainability, which together lead the way to the revitalization of supersonic commercial aviation. Because no competitor has yet succeeded in addressing all of these criteria, Goldeneye AB1 seeks to spearhead the effort and in so doing establish itself as the front-runner in this promising- industry.

2 Wing

2.1 Overview

The crowning feature of Goldeneye AB1's design lies in its wing, both figuratively and literally. Throughout the history of supersonic aviation, the greatest challenge has been posed by poor aerodynamic wing efficiency. This is primarily due to the fact that it has proved very difficult to design a wing with a low drag coefficient that simultaneously produces sufficient lift at these speeds. Many different wing configurations have been employed in efforts to achieve this, from the Concorde's classic ogival delta wing to the swept and arrow wings of various supersonic military jets. Notably, the tapered trapezoidal wings of early experimental planes such as the Lockheed F104 and Douglas X-3 yield improved performance at supersonic speeds. While Goldeneye is primarily a supersonic aircraft, it is designed for optimal performance at both subsonic and supersonic speeds, something that has never been done before. To accomplish this requires looking into both the past and present, studying prior wing configurations as well as modern ones. What results is a stunning compromise that pays homage to the past while simultaneously trailblazing a new path for supersonic flight into the future.

Unlike any other variable geometry aircraft, the AB1 is equipped with radially extending panels stowed inside the rear portion of each wing. During subsonic cruise as well as takeoff and landing, these panels are fully extended, forming an ogival delta wing reminiscent of the Concorde's. At supersonic speeds the sector-shaped panels rotate inward about pivots positioned at the back of each wing, adjacent to the fuselage, which transforms the wing into a clipped ogival delta shape (See Figure 1 below). This is discussed extensively in Section 2.4.

2.2 Aerodynamic Theory

An airfoil that performs well at supersonic speeds is a baseline for AB1's success. The NACA 66-206 airfoil is a perfect choice for several reasons. First, it reduces wave drag caused by shock waves that rapidly form as the plane approaches transonic speeds (incidentally, this sudden spike in drag is what creates the sound
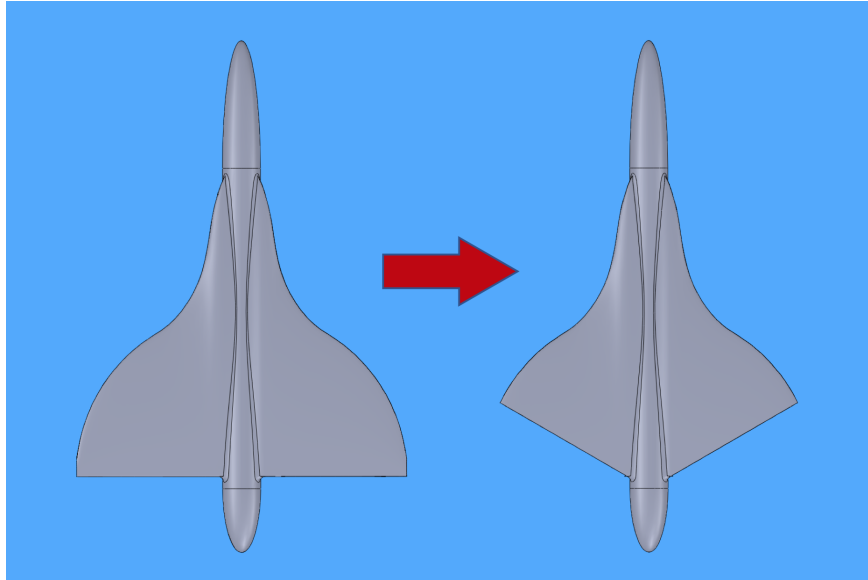
Figure 1: Goldeneye AB1 transforming its wing from an ogival delta to a clipped delta shape.

barrier) [1]. Second, the airfoil has a higher chord to camber ratio than many other supersonic airfoils, which implies a large surface area for lift at supersonic speeds. Finally, it has a relatively small coefficient of lift at small angles of attack (α), as demonstrated by the plot in Figure 3 on the following page. This reduces the turbulence that the wing experiences during supersonic cruise, ensuring that laminar flow is maintained, which further reduces drag.

During supersonic cruise, the clipped delta wing reduces aerodynamic shear stresses on the surface of the airfoil, enabling the profile of the wing to be thinned. This in turn allows for sharp leading and trailing edges, significantly reducing the wing's drag coefficient. However, during subsonic cruise this wing shape is less aerodynamically efficient and fails to generate sufficient lift. Given the 7,000-meter runway limit, Goldeneye is confined to using existing airport infrastructure and therefore requires the full delta wing in order to provide enough lift to take off and land at subsonic speeds. With its panels fully extended, the wing induces vortex lift [2], a phenomenon that occurs with a swept back wing at high angles of attack. The sharply swept leading edge of the wing induces turbulence that generates vortices across the chord of the wing from the leading edge toward the trailing edge. These vortices are trapped by the outside air, which flows around them and down the back of wing, generating additional lift. The panels supply more wing surface area for the turbulent airflow to act upon, generating additional vortex lift required for flight. Rather ingeniously, the variable geometry of AB1's wing serves to optimize aerodynamic efficiency at both subsonic and supersonic speeds, drastically improving the plane's performance and pioneering a new era of variable geometry in aviation.
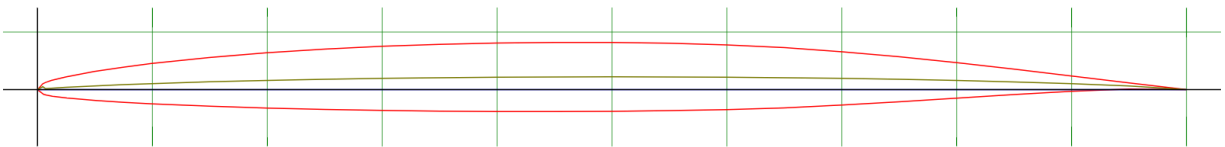

Figure 2: The highly laminar NACA 66-206 Airfoil. Its slight camber and thin profile renders it a good choice for the AB1's wing.
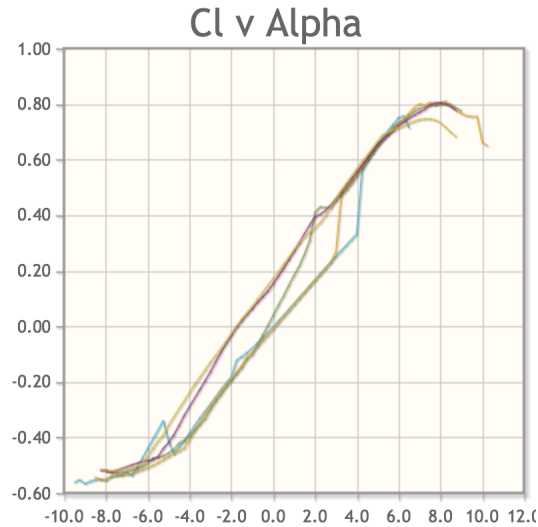
Figure 3: NACA 66-206's lift coefficient (y-axis) vs. attack angle (x-axis) for various Reynolds numbers [15]. At low angles of attack, the coefficient of lift is correspondingly small, a desired trait for a supersonic wing.

2.3   Wing Design Parameters

As previously mentioned, clipped delta wings have been demonstrated to induce less drag than more conventional delta wing geometries at supersonic speeds, making them more efficient in this regard. However, a critical problem for a clipped delta wing at supersonic speeds is its comparatively low lift in the subsonic region. This stems from the fact that the clipped wing has lower planform area than a normal delta wing with the same span and root chord. Many other supersonic wing designs, such as the supersonic laminar trapezoidal wing [3], struggle with the same issue. Since the wing area is decreased, a greater velocity is needed for takeoff, which requires more thrust and consequently increases the amount of noise generated at low altitudes, a major concern for Goldeneye.

Fortunately, the AB1's variable wing geometry allows for the clipped delta wing to be used for supersonic flight, while employing the full ogival delta wing while flying at speeds under the sound barrier, including takeoff and landing. The mechanism by which this is made possible is elaborated upon in Section 2.4.

2.3.1   General Design Parameters

The first parameter considered in the wing design is the vertical placement of the wing. Since the chosen airfoil is laminar, the primary goal of the vertical placement is to maintain streamlined airflow along the wing. A mid-fuselage placement, halfway up the fuselage's height, is more aerodynamically efficient than an upper or lower blend because it reduces interference drag along the wing. [4]. An added benefit of this configuration is that it keeps the wing closer to the top-mounted engines where it can deflect more of the engine noise away from the ground than a lower mounted wing without being exposed to the high-temperature exhaust gases that an upper wing would experience. The additional support structure required for the mid-fuselage configuration is housed in the edges of the elliptical fuselage outside of the cabin, which is further discussed in Section 3. Modern materials such as carbon fiber composites minimize the extra weight of this more involved structure, making it worthwhile.

Because the drag experienced by the wing increases with wing span dramatically, especially when the wing intersects the Mach cone, a low aspect ratio for the wing is desirable. Furthermore, due to the unique design challenges posed by the variable wing geometry, it is not feasible to implement an angle of twist or dihedral angle that varies along the wing's cross section. Fortunately, this does not pose an issue because these angles are typically small, if not zero, for laminar supersonic wings [5]. In fact, these wings often have zero incidence angle as well to avoid flow separation [6].

2.3.2 Oblique Shock

Though the NACA 66-206 airfoil is highly laminar, oblique shock waves can nevertheless induce large amounts of wave drag on the wing when the critical Mach number is exceeded. The sweep angle of the wing must be designed to avoid these issues as much as possible. The angle of the oblique shock wave is given by [7]:

$$\mu = \sin^{-1} \frac{1}{M}$$

Where M is the Mach number. At Mach 1.7, the average desired cruise speed, this angle is 36 degrees. The sweep angle should be slightly larger than necessary to guarantee minimal shock wave interaction [7]. Therefore, the sweep angle Λ is chosen with a 10% buffer to be:
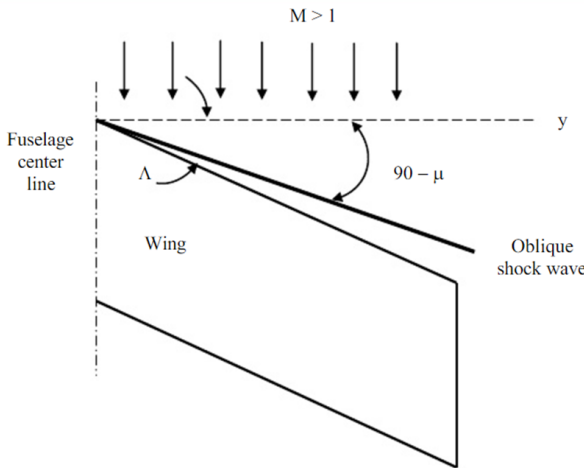
$$\Lambda = 1.1(90° - \mu)$$

Figure 4: Diagram of a wing with μ, Λ, and oblique shock wave at speeds higher than Mach 1 [7].

This results in a sweep angle of $59.3 \approx 60$ degrees. Similar consideration must be given to the trailing edge, where the wing's disturbance may result in oblique shock waves impacting points farther along the trailing edge. Because the clipped delta wing is symmetric across its span, the elegance in its design lies in the fact that both the leading and trailing edge approach but do not cross into the zone where oblique shock waves form. Not only do disturbances in flow influence the wing downstream, they may also carry this influence upstream, bounded by the same μ angle [8]. These effects are minimized when the clipped delta wing approaches the oblique shock angle, increasing the stability of the flow. The rear sweep angle can still be decreased to optimize lift when Goldeneye's wing is extended into the full delta geometry. The flow and shock waves along the trailing edge are not negligible because the regions of highest flow velocity around the NACA 66-206 airfoil lie near the trailing edge (See Figure 5 on the following pagr). However, if the trailing sweep angle is less than 60 degrees, the radial extension cannot be fully stored within the main wing. Therefore, the minimum trailing sweep angle is constrained to 60 degrees, which can be increased to generate more supersonic lift.

2.3.3 Whitcomb Area Rule

The Whitcomb Area Rule states that in the transonic velocity region, the gradient of the frontal cross sectional area must be minimized to decrease drag and shock wave effects [10]. This logic applies to the supersonic region to a certain extent as well. To quantify this statement mathematically, if the area is to change at all, then one must find a representative distribution for the area $A(x)$ with respect to distance along the wing parallel to the fuselage axis such that its derivative is minimized at all points along the length of the fuselage, that is:

$$\{A(x) \mid \frac{\mathrm{d}A(x)}{\mathrm{d}x} = \frac{\mathrm{d}A(x)}{\mathrm{d}x}|_{\min} \ \forall \ x \in (a,b)\}$$

Where a and b denote the start and end points of the aircraft fuselage, measured on the x-axis. To satisfy for the area rule, the transition from fuselage to wing must be as smooth as possible. Therefore, a cubic spline $y = ax^3 + bx^2 + cx + d$ is fitted to the leading edge. The spline is constrained to lie between the points $A(0,0)$ (where the front of the wing meets the fuselage) and $B(x_b, y_b)$ (the outermost tip of the clipped wing's span, where it changes direction back toward the fuselage). This complex analysis may be confusing, so Figure 6
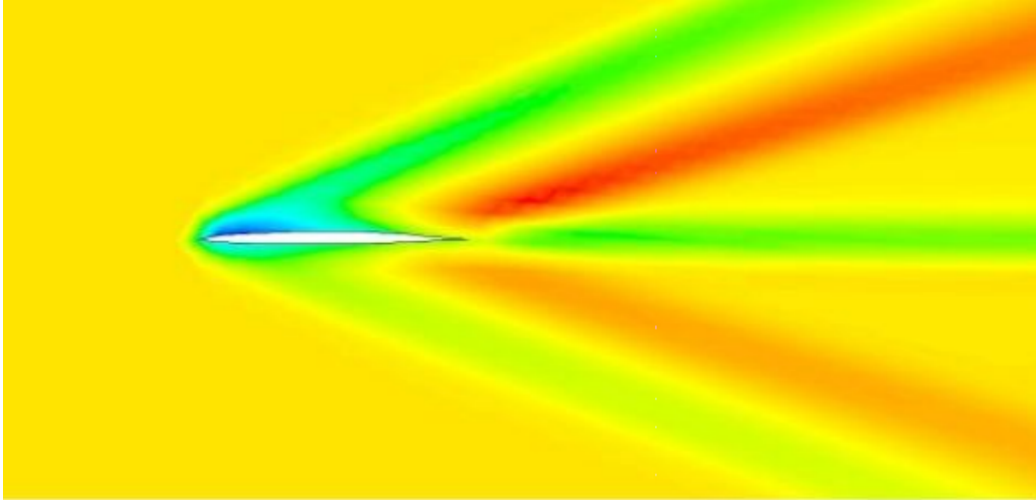
4

Figure 5: Mach number variation over NACA 66-206 airfoil at Mach 2 [9]. Red represents the highest speeds while blue represents the slowest.
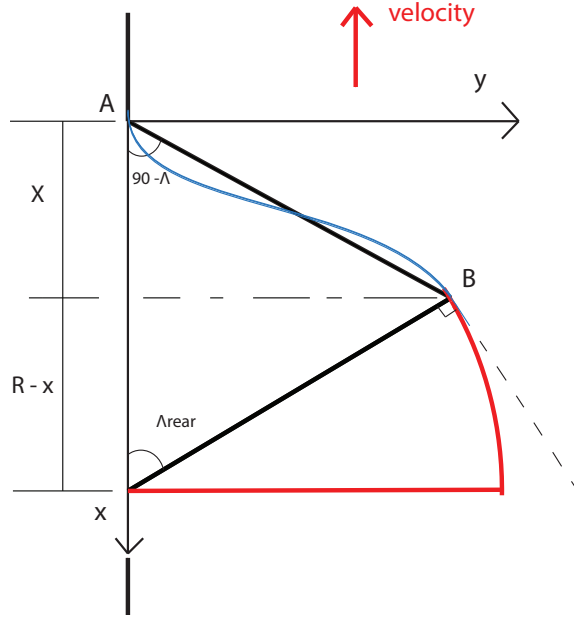

Figure 6: Coordinate System for the Whitcomb Area Rule problem.

is included to improve comprehension. Additionally, the derivative of the spline is constrained to be equal to the slope of the fuselage at A, and to smoothly blend with the radial extension at point B. This forces the wing profile at B to be normal to the slope of the trailing edge, giving

$$x_b = \frac{R \tan(\Lambda_{\text{rear}})}{\tan(\Lambda_{\text{rear}}) - \tan(90 - \Lambda)} \qquad y_b = x_b \tan(90 - \Lambda)$$

Where R is the root chord of the wing. Summarizing these constraints:

$$y(0) = 0 \qquad y(x_b) = y_b \qquad \frac{\mathrm{d}y(0)}{\mathrm{d}x} = 0 \qquad \frac{\mathrm{d}y(x_b)}{\mathrm{d}x} \tan(\Lambda_{rear}) = -1$$

5

Solving the equations, the result is that $c = d = 0$ and:

$$\begin{bmatrix} x_b^3 & x_b^2 \\ 3x_b^2 & 2x_b \end{bmatrix} \begin{bmatrix} a \\ b \end{bmatrix} = \begin{bmatrix} y_b \\ 1/\tan(\Lambda_{rear}) \end{bmatrix}$$

This provides a straightforward way to solve for the leading edge spline function with respect to the root chord and rear sweep angle. Now there is a solid framework to prototype the wing; the rear sweep angle can be increased or decreased to optimize the subsonic lift (as it changes the area of the radial wing extension), and the root chord can be increased to boost overall size and lift.

A well-documented benefit of highly swept wings is their induced dihedral effect, summarized succinctly:

> "A swept wing produces a negative rolling moment because of a difference in velocity components normal to the leading edge between the left and right wing sections, hence, a swept wing may not need a dihedral or anhedral to satisfy lateral-directional stability requirements" [11].

2.3.4   Center of Pressure Optimization

There are a number of other perks generated by the ability to switch from a clipped delta to a full delta wing shape. One of these presents itself when tackling one of the major design concerns faced by the Concorde: its shifting center of pressure. As aircraft velocity increases, the wing's center of pressure shifts backward, toward the trailing edge. As such, the center of pressure of the Concorde would shift around 6 feet between takeoff and supersonic cruise [12]. To account for this, an elaborate fuel pumping control system was designed to distribute fuel mass to move the center of gravity of the aircraft and maintain stability. This greatly complicated the design, increasing cost as well as necessitating the energy required to pump 20 tons of fuel around the plane.

This issue is circumvented by the variable wing geometry as the radial extension increases pressure near the trailing edge of the wing at low speeds, moving the center of pressure backward. Since the extension retracts during supersonic flight, the loss of this added pressure offsets the natural rearward displacement of the pressure center at supersonic speeds. The result is a design that can be optimized to keep the center of pressure in approximately the same location at both subsonic and supersonic velocities. Mathematically, the wing is designed such that:

$$\frac{\iint_{S_1} x \cdot P_{\text{super}}(x,y)\mathrm{d}x\mathrm{d}y}{\iint_{S_1} P_{\text{super}}(x,y)\mathrm{d}x\mathrm{d}y} = \frac{\iint_{S_2} x \cdot P_{\text{sub}}(x,y)\mathrm{d}x\mathrm{d}y}{\iint_{S_2} P_{\text{sub}}(x,y)\mathrm{d}x\mathrm{d}y}$$

where P_{super} and P_{sub} are the pressure distributions along the wing at supersonic cruise and a representative subsonic velocity, S_1 is the clipped delta wing planform area, and S_2 is the full delta planform area [13]. .

2.3.5   Thickness Ratio Optimization

Another benefit of the variable wing geometry is the opportunity to change the thickness ratio of the airfoil. Since the extension is stored within the wing, as soon as it is deployed, the hinges on the trailing edge of the clipped wing open to allow the extension to protrude farther (see Section 2.4). Therefore, the 6% thickness ratio of the NACA airfoil can be changed during subsonic flight. The ideal thickness ratio for that condition is governed by the Torenbeek equation [14]:

$$\frac{t}{c} = 0.30\left[\left(1 - \left(\frac{5 + M^2}{5 + (M^*)^2}\right)^{3.5}\right)\frac{\sqrt{1 - M^2}}{M^2}\right]^{2/3}$$

Where $\frac{t}{c}$ is the thickness ratio, M is the Mach number, and M^* is a constant unique to each airfoil profile. This allows the extension-modified airfoil to have a thickness ratio optimized for any subsonic Mach number.

2.3.6   Wing Comparisons

One final comparison is noteworthy enough to be drawn between the proposed clipped delta wing, the Concorde's full delta wing, and the laminar trapezoidal wing of the Aerion and Boom supersonic aircraft. The full delta geometry of Goldeneye's wing is extremely similar to the ogival delta wing of the Concorde. However, the Concorde's wing is often categorized as a variable sweep wing, which struggled to balance supersonic and subsonic efficiency. The Aerion's laminar trapezoidal supersonic wing provides less lift at subsonic speeds, which bears responsibility for undesirable noise, runway, thrust and weight characteristics. However, the Aerion demonstrates that, given a highly laminar airfoil, oblique shock waves are perhaps not quite as significant a concern. This means that the front sweep angle can be tweaked as well in finalizing a scaled version of the wing to suit the lift requirements of the aircraft. Thus, Goldeneye's variable geometry wing cleverly manages to capture the best of all worlds.

2.4   Mechanism

Historically, aircraft variable wing geometry has proved costly and technologically complex. Previous mechanism designs often malfunctioned, broke, or had such fundamental flaws that their production was discontinued. Most variable geometry designs consist of a single pin joint several feet outboard of the fuselage about which the entire wing rotates. This implementation is structurally vulnerable because it subjects the pin to immense shear stress from the moment created by the weight of the fuselage and the wing's lift force.

Goldeneye's design seeks to eliminate this common design flaw. Similar to a Fowler flap [16], the panel is secured with rollers that are fixed to its bottom side and slotted into two radial tracks grooved into the bottom of the interior of the wing. To move the panel, a straight groove in the top of the wing interior houses a linear hydraulic actuator that is attached by pivots to the foremost straight edge of the panel on one end and to the edge of the wing, adjacent to the fuselage, on the other end. As the aircraft transitions between subsonic and supersonic cruise, the actuators retract or extend within their grooves, rolling the panel along the curved tracks radially until the desired wing shape is reached (see Figure 7 below).
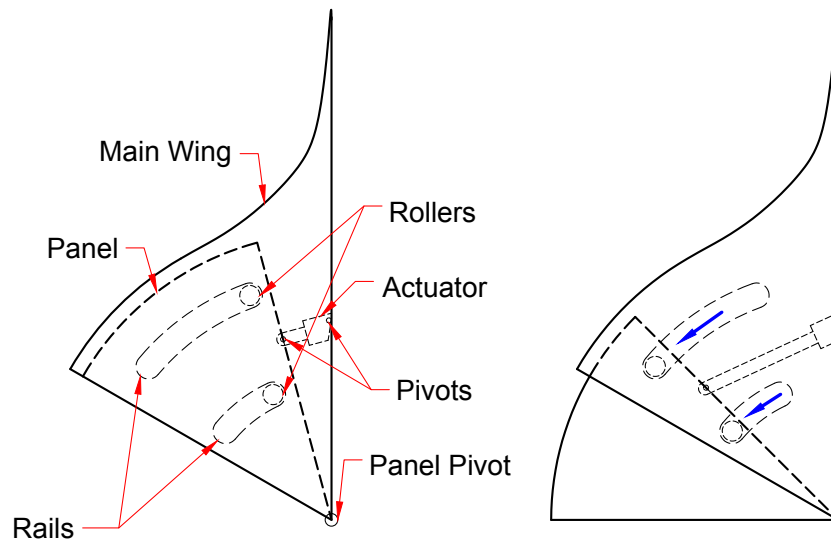

Figure 7: Top view of the left wing, revealing the interior design of the radial panel mechanism as it extends outward. Wing shape and mechanism size not to scale.

To allow for this motion, the trailing edge of the clipped wing has thin flaps that are hinged to the back of the wing at the highest and lowest points of the clipped face for ease of motion. These hinged flaps allow the

end of the interior channel to narrow or widen to accommodate the increasing or decreasing thickness of the exposed region of the panel. This maintains a smooth curve so as not to disrupt airflow over the wing.
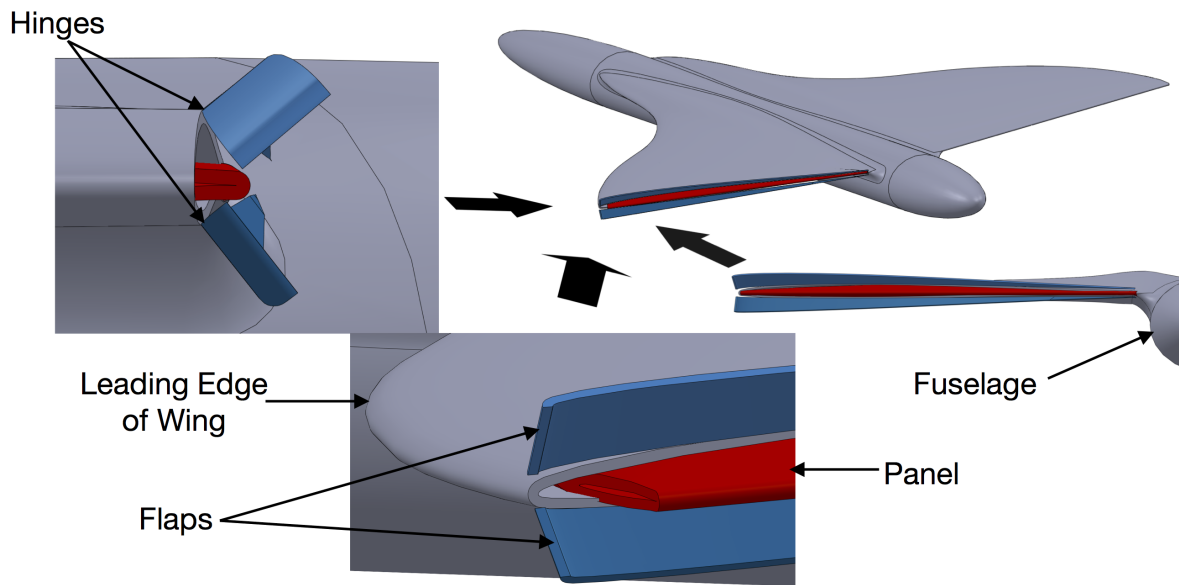
(a) Panel retracted, with hinges opened to allow for extension.
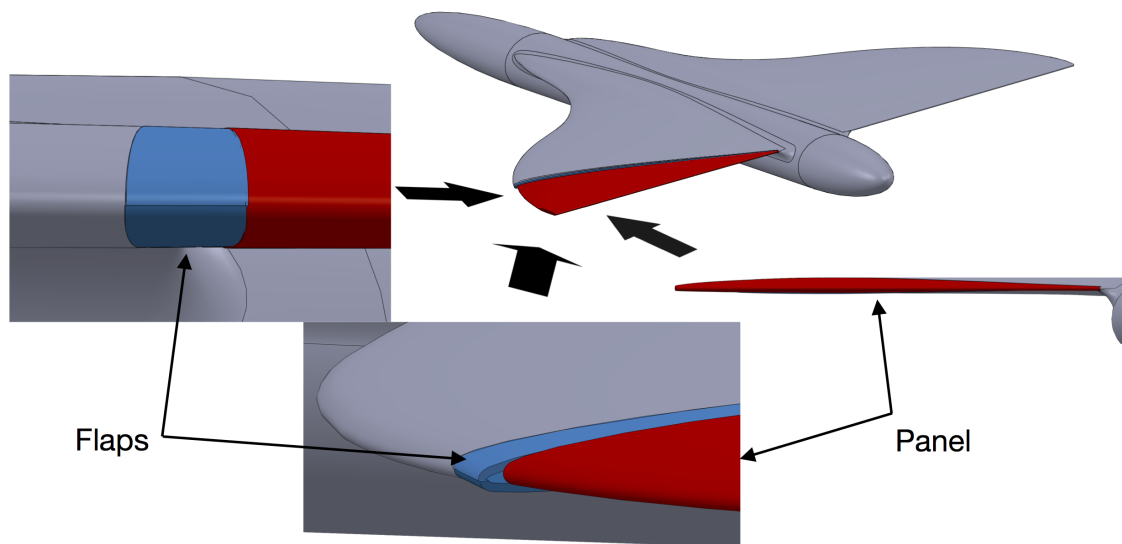
(b) Panel extended, with hinges closed to maintain smooth wing surface.

Figure 8: Side, oblique, and back views of the panel, depicted as it extends outward. Note that the panel starts slightly extended from the wing's channel even when fully retracted.

To preserve the airfoil's shape, the panel is designed such that it serves as the back of the airfoil when fully extended, complementing the front of the airfoil from the fore region of the wing. This requires that the panel's airfoil axis be parallel to the fuselage's when it is fully extended. Consequently, when the panel is fully retracted, its airfoil axis is offset from the fuselage's by the angle between the trailing edge of the clipped wing and a line perpendicular to the fuselage. This issue is resolved by installing the panel such that it is always at least slightly extended from the wing interior, even when retracted (See Figure 8 on the previous page). It should be noted that the trailing edges of the main wing and panel remain adjacent when the panel is fully retracted, and that the hinged flaps lie just on top and bottom of the panel's trailing edge in this configuration. In this way, Goldeneye's wings have a smooth, continuous airfoil at all times.

2.5 Control Surfaces

One of the main concerns arising from the use of variable geometry wings is how to implement the control surfaces that roll and pitch the aircraft. Conventionally, ailerons are mounted on the trailing edge of the wing to control the rolling moment. However, this configuration is only possible for Goldeneye during subsonic flight. This is because the radial panel is only extended at low speeds and ailerons may only be placed on the trailing edge of the panel since the main wing features hinged flaps that preserve the airfoil's shape. While roll control is most important during subsonic flight when AB1 does the majority of its maneuvering, it will spend much time at supersonic cruise, making it necessary to better control AB1's unstable roll. To address this problem, inspiration can be gleaned from the Grumman F-14, a supersonic fighter jet with variable-sweep wings. This aircraft uses wing-mounted spoilers instead of ailerons to enable roll control, even during supersonic flight. However, the spoilers must be disabled if the plane's sweep angle exceeds 57° [17]. Fortunately, Goldeneye's variable geometry does not affect its sweep angle, allowing the installation of wing spoilers that are functional during both subsonic and supersonic flight.

The Concorde had the luxury of ailerons as a primary control surface, operating them differentially to generate a rolling moment and symmetrically for a pitching moment. Furthermore, it did not require a horizontal stabilizer due to the added stability of the delta wing at supersonic speeds. On the contrary, Goldeneye is much less horizontally sound during supersonic cruise because of its clipped delta wing, trading stability for reduced drag. Therefore, a separate mechanism is required for both horizontal stability and to control pitch, which the spoilers do not address. A canard seems to be the simplest and most effective way to achieve this, discussed further in Section 5.2.

2.6 Materials & Structure

The wing's frame consists of tapered steel cross sections joined by two titanium spars. Its surface is coated with aluminum alloy 7075-O, a common industry-grade aviation material. The steel tracks for the extension mechanism are attached to the wing's cross-sections via titanium fasteners, atop which the radial panel rests. The panel is comprised of carbon composite cross sections united by a spar to reduce weight and is stored in the empty space between the wing's cross sections.

3 Fuselage

3.1 Cabin

The length and cross-sectional area of Goldeneye AB1's cabin is dictated by the passenger load for which the plane is designed. Holding up to 12 passengers, Goldeneye's cabin is an elliptical prism measuring 3 meters along its major axis, 2.4 meters along its minor axis, and 10 meters in length, with a shell thickness of 2 centimeters. The floor is positioned 2 meters (6.56 feet) below the apex of the cabin for optimal headroom. The elliptical cross section serves to maximize passenger space inside the cabin while still leaving space for the mid-fuselage wing mount connections. In addition to providing more volume for storage of luggage and other cargo (relatively small loads for a business jet), this shape also provides for a more seamless integration with the wing mount than with an upper or lower fuselage blend, which is not only more aesthetically pleasing but also reduces interference drag due to the interaction of airflow streamlines between the wing and fuselage [19].

Underneath the cabin, AB1's underbelly serves primarily as fuel storage. Because it is a business jet, Goldeneye is not concerned with providing excess cargo space, though the very front of the underbelly features a sizable volume for this purpose. Aft of this space, three equally sized fuel tanks line the rest of the underbelly, adjacent from front to back. The tanks are connected by valves to control the drainage rate. Normally, the tanks empty evenly in order to keep the plane's center of gravity stable, but this can be adjusted accordingly if need be.

3.2   Nose and Tail

Goldeneye's fuselage is designed around the aerodynamic principles governing supersonic flow in order to minimize drag at supersonic speeds. The nose and tail are both formed from half of a Sears-Haack body, mounted directly fore and aft of the cabin, respectively.

The Sears-Haack body is a geometric shape that theoretically minimizes wave drag in supersonic flow for a given length [20], making it a perfect choice for Goldeneye's nose and tail. These features differ from the ideal Sears-Haack half body in that their cross sections are elliptical instead of circular. Fortunately, this does not alter their construction process too drastically. The equation for the radius of a circular Sears-Haack cross section is given by:

$$r(x) = R_{\max} \left[\frac{2x}{L} \left(1 - \frac{x}{2L} \right) \right]^{3/4}$$

where x is the distance from the tip of the half-body, L is the length of the half-body, and $R_{\max}$ is the maximum radius of the half-body, taken to be the semi-major axis of the fuselage (1.5 meters) to ensure that the components mesh together smoothly. First, the nose and tail lengths are chosen. Then, to preserve the cross sections as ellipses, $r(x)$ is used to calculate the semi-major axes of the cross sections at set intervals. The full ellipses are constructed by fixing their eccentricity at the same value as the cabin ellipse, which is found by $e = \sqrt{1 - \frac{b^2}{a^2}} = 0.6$, where a is the semi-major axis (1.5 meters) and b is the semi-minor axis (1.2 meters). Finally, the cross sections can be connected into one smooth shape by a loft (Figure 9 below).
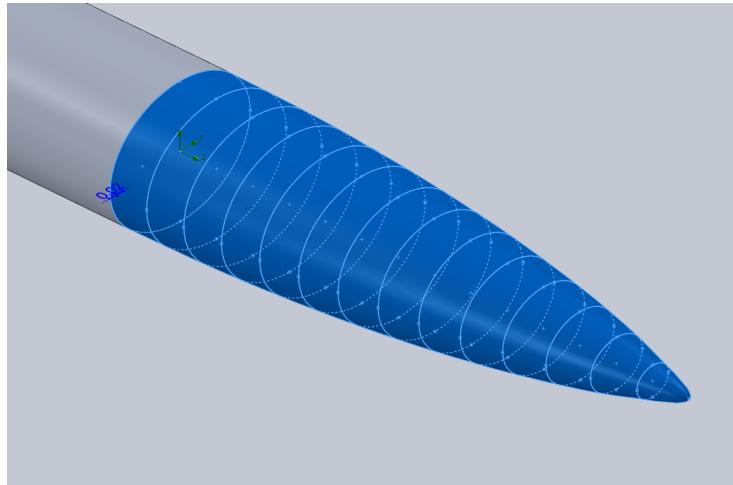

Figure 9: Fusing a 10m nose to the fuselage by lofting ellipses at regular intervals.

Now all that is needed are lengths for the nose and tail, whose optimal values can be determined from flow simulations. As expected, the longer the Sears-Haack body, the more gradually it tapers to a point and the less drag present. However, this also incurs more weight and therefore more lift required, so a decision must be made to compromise between the two. Because the plane will spend the majority of its flight time traveling at supersonic speeds, drag should be minimized for a Mach number of 1.7, the mean target speed for the

aircraft. Assuming that Goldeneye travels at an altitude of 18,000 meters, roughly the maximum height at which the Concorde flew, the average air pressure and temperature would be about 7500 pascals and 215 Kelvin, respectively. Inputting this information into the simulation parameters and arbitrarily fixing the tail length to 5 meters, we can compare the average drag force on the entire fuselage to the volume of the material making up the nose, since volume has a one-to-one correspondence with mass, regardless of material. This allows for the fuselage material to be determined later. The more voluminous the nose, the more lift will be required for the plane to fly. Plotting the results averaged after 5 trials for each nose length at 1-meter intervals from 7 to 12 meters, the relationship between these properties appears to be best modeled by a cubic function in this range, displayed by the plot in Figure 10a below.
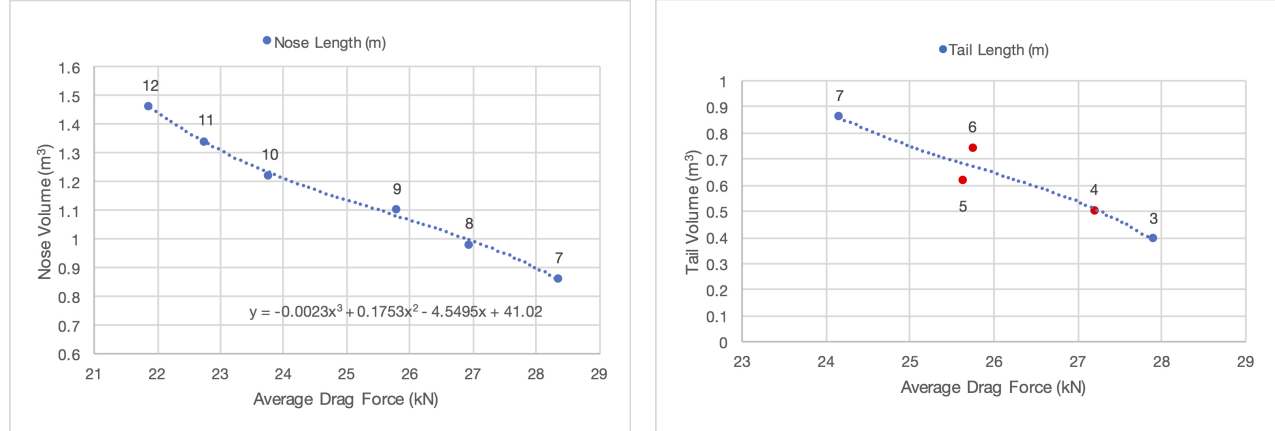
(a) Nose volume vs. average fuselage drag force for various nose lengths with a fixed 5-meter tail.

(b) Tail volume vs. average fuselage drag force for various tail lengths with a 9.2-meter nose. Red data points illustrate that the properties are not related by a function.

Figure 10: Plots depicting the results of the flow simulations to determine optimal nose and tail length.

The nose length corresponding to the inflection point of the cubic function is the best choice for the fuselage because beyond this nose length the mass begins to increase more significantly rapidly as drag decreases. This point can be found by finding the root of the function's second derivative, which corresponds to a value of 25.41 kN. Finally, using our drag values to interpolate between the 9-meter and 10-meter nose lengths the optimal nose length is found to be 9.2 meters.

Now that we have a fixed nose length, the same analysis can be performed to find a corresponding optimal tail length. Running the flow simulations with the same environmental properties and a 9.2-meter nose, the average drag force can be calculated in a similar manner at 1-meter intervals for tail lengths from 3 to 7 meters. Interestingly, when the drag values are plotted against the tail volume, the relationship between these values is not the same as with the nose. This is likely due to the nose interfering with the flow before it reaches the tail and therefore perturbing the results. Unfortunately, the data do not appear to be modeled by any function, since the drag force decreases from the 4-meter to the 5-meter nose, but then increases when the nose is extended to 6 meters (Figure 10b above). One can quickly see that no matter how the points are connected, the plot fails the vertical line test (the data points of interest are highlighted in red). Without a clear understanding of the relationship between the drag and the tail volume, the most logical choice for the tail length can only be based on the experimental data, which suggests choosing a point in the vicinity of the 5-meter tail, where the drag is lower than expected based on the rest of the plot. Setting the tail length to 4.8 meters, the overall length of AB1 is a nice round 24 meters.

3.3 Cockpit

The cockpit is simply an extension of the cabin, ending where the cabin floor meets the nose when extended forward. The bottom dimension is thus preserved, meaning that the perpendicular distance from the cockpit floor to the cabin apex is still 2 meters. However, the cockpit roof must conform to the top of the nose,

tapering down until it reaches the same forward distance as the floor. The resulting loss of head space does not pose an issue since the pilot and co-pilot are seated at all times inside the cockpit. Unlike the Concorde, AB1's windshield is seamlessly integrated with the nose to preserve the Sears-Haack shape and minimize drag at a minimum. At high angles of attack during takeoff and landing, this design poses a visibility issue. To avoid a complicated and expensive design like the Concorde's droop nose, Goldeneye is equipped with cameras to aid the pilot, a simple solution to an important problem.

3.4 Materials

The skin of an aircraft, especially on the fuselage, experiences extreme shear stresses and temperature fluctuations during flight. Thus, materials making up the external structure of an aircraft are characterized by creep resistance, high tensile strength, and a low thermal expansion coefficient. Furthermore, they must not be very dense to reduce the weight of the frame. Traditionally, aluminum alloys have been used in these applications as they possess many of the aforementioned characteristics.

However, supersonic flight poses additional challenges. To reach such high speeds, supersonic aircraft must fly at higher altitudes than their subsonic counterparts in order to take advantage of the thinner atmosphere. This creates larger hoop and radial stresses within the fuselage, as well as much higher thermal stresses due to the adiabatic compression of the incoming air.

For these high performance requirements titanium alloys make good candidates, namely, Ti-6Al-4V. This alloy has a very desirable strength-to-weight ratio, a low thermal expansion coefficient, and significant fatigue resistance. Additionally, it is highly resistant to corrosion. In order to enhance the strength of the alloy, it may be nitrided to produce a case-hardened surface, which preserves the alloy's ductility under bending moments while improving its fatigue resistance by introducing compressive stresses at the surface that limit the rate of crack growth.

Ti-6Al-4V is chosen to construct Goldeneye's fuselage over other alloys, including Hiduminium, Al-Sc alloys, and 7068 aluminum, due to its superior tensile strength and lower cost. The alloy is most critically needed near high-stress areas of the airframe, such as the wing root, nose tip, and engine casing. In areas where stresses are generally lower, it may be permissible to employ other alloys to reduce weight at a slight cost of strength. For example, Hiduminium, along with other aluminum alloys such as 6061, is perfectly suitable for structural components within the fuselage. Struts, supports, and other features within the aircraft are not impacted by environmental factors, and therefore the selection criteria for these parts is less rigorous.

Composite materials, especially laminates and sandwich panels, may serve a purpose in the fuselage as well. Sandwich-structured composites and fiber-reinforced polymers have the ability to produce very strong materials, but also come with several drawbacks. The construction of sandwich panels and fibrous composites in a matrix implies that the material is much weaker in one direction. For example, care must be taken to ensure that the facesheets of a sandwich panel do not detach from the core. The mechanical properties of fiber-reinforced epoxies vary greatly depending on whether the applied stress is parallel or perpendicular to the direction of the fibers. Therefore, unless the full extent of the loading condition is considered beforehand through much deeper analysis, it is impractical to rely heavily on such materials.

4 Propulsion

Goldeneye's propulsion system is modeled after an existing engine, which is first scaled to fit on the plane and then tweaked to improve performance. The engine of choice is the Olympus 610 of the Concorde B, an improved but unfinished revision of the original Concorde's design. This engine is one of only two ever successfully built to propel a supersonic commercial plane[1]. Olympus 610 is the result of years of research and development to optimize long-range engine performance, which addresses the low-range barrier that most other supersonic propulsion systems face, making it a good starting point to scale into an analog engine for Goldeneye.

---

[1]The other supersonic commercial jet was the Kuznetsov NK-144 of the Russian-manufactured Tupolev Tu-144

4.1 Engine Dimensions & Supersonic Thrust Calculations

A number of scaling arguments are used to tailor the Olympus engine to Goldeneye's fuselage and wings. Given the much smaller size of the plane relative to the Concorde, a two-engine setup makes the most sense as opposed to the Concorde's four-engine layout.

The following arguments are included to mathematically justify the engine scaling process [21]:

$$s = \frac{T_{\text{reqd}}}{T_{\text{data}}} \qquad L_{\text{reqd}} = L_{\text{data}} \cdot s^{0.4} \qquad D_{\text{reqd}} = D_{\text{data}} \cdot s^{0.5} \qquad W_{\text{reqd}} = W_{\text{data}} \cdot s^{1.1}$$

$s \equiv$ Scale Factor $\qquad\qquad\qquad$ $L \equiv$ Engine Length
$D \equiv$ Engine Diameter $\qquad\qquad$ $W \equiv$ Engine Weight
$T \equiv$ Thrust

where the subscript reqd represents values for Goldeneye's engine and data represents values for the Olympus engine.

To calculate the dimensions of the scaled engine, an estimate of the thrust during level flight is required, which can be found by [23]:

$$T_{\text{reqd}} = \frac{W}{C_L/C_D}$$

where C_L is the lift coefficient and C_D is the drag coefficient.

To account for deviations from the ideal conditions that the previous equations assume (a constant drag force that does not account for the plane's acceleration), the theoretical required thrust is calculated for the Concorde. Observing that this formula underestimates the required thrust by 11.98%, a correction can be made to more accurately calculate Goldeneye's required thrust:

$$T_{\text{reqd}} = 1.1198 \cdot \frac{W}{C_L/C_D}$$

Because Goldeneye's weight is a bit vague due to different materials considerations, it is a good idea to use a similarly sized subsonic plane, the Gulfstream G280 [24], to provide an upper bound for Goldeneye's weight (18000 kg). The coefficient of lift (0.125) and drag (0.0175) are taken from the Concorde's supersonic cruise as a worst-case estimate, since the fuselage and wings of Goldeneye are more optimized for streamlined flight than the Concorde's. Plugging these numbers in, it is calculated that $T_{\text{reqd}} = 21722$ N and therefore both engines must supply at least half this thrust, 10861 N. Finally, with this value the scaling factor and specifications of the engine are found to be:

$$s = 0.2395 \qquad L_{\text{reqd}} = 3.34\,\text{m} \qquad D_{\text{reqd}} = 0.684\,\text{m} \qquad W_{\text{reqd}} = 660\,\text{kg}$$

where L_{reqd}, D_{reqd}, W_{reqd} are the length, diameter and weight of each engine, respectively.

4.2 Afterburner Performance

Planes with the ability to supercruise, that is, to fly at supersonic speeds without an afterburner, may or may not employ an afterburner to ease the surpassing of the sound barrier. This is an substantial decision to make because the use of an afterburner drastically increases fuel consumption. However, the advantage of an afterburner is that it shortens the duration of time required to break the sound barrier. As Figure 11 on the following page indicates, most supersonic airfoils experience a sharp increase in drag as the plane approaches the speed of sound, followed by a rapid decline in drag [26]. Consequently, many supersonic planes do have

afterburners because the time saved as the plane transitions from subsonic to supersonic velocity (Figure 12 below) makes up for the short, intense burst of fuel consumption and actually conserves fuel overall. This phenomenon is illustrated by the plots below and suggests that Goldeneye should employ an afterburner to break the sound barrier more efficiently.
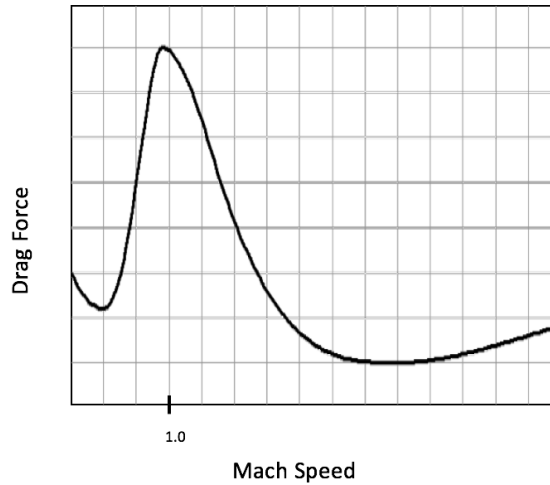

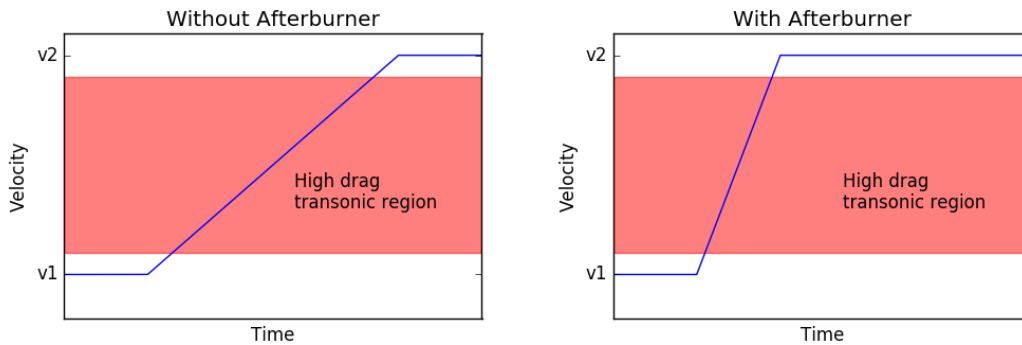Figure 11: Drag vs. Mach number for a typical supersonic jet [26].

Figure 12: Plane velocity vs. time elapsed while breaking the sound barrier without and with an afterburner.

4.3 Inlet

Recent supersonic designs feature intake ramps because of their adaptability over vast ranges of conditions, angles of attack, and mass flows. The variable ramp offers short-term high efficiency propulsion over a wide extent of supersonic speeds. This is an important characteristic for fighter aircraft because they often perform sharp maneuvers, and may accelerate to supersonic speeds for minutes at a time. Under these circumstances, air mass spill is severe, often causing shadows and gaps to form in the airflow due to directional changes. This need for adaptability makes the high weight and complexity of ramp inlets worthwhile.

With that being said, a supersonic business jet's main function is to sustain supersonic cruise for long periods of time, not short intervals. For this reason, Goldeneye's inlet design consists of a moderate spike intake featuring a conical section the extends forward from the inlet of the engine. This feature is advantageous for several reasons: it does not disturb airflow to the engine, is lightweight and compact, and reduces construction

14

and maintenance costs. Furthermore, while it may be extensive, because the ducting's sole purpose is to separate the interior and exterior flow, the engine can be quite lengthy without significant increases in drag or weight.

The inlet resembles those of the MiG-21 or SR-71 engines, so the forward end of the engine can be modelled as a cylinder with a conical spike. Though past aircraft with engines situated inside the fuselage (such as the Mach-2-capable English Electric Lightning) have used the cone to store radar equipment, Goldeneye's is hollow for weight reduction. In addition, the radar's performance is heightened when it is placed father forward in the aircraft. A simple translational mechanism moves the cone back and forth to adjust the intake cross section. To provide a shallow angle of attack, the cone length is 3 meters and cone radius is 0.335 meters, which is almost completely inside of the 4-meter long ducting area when retracted. At subsonic speeds, the retracted cone compresses the mass that flows into the frontal section, which then passes into the engine cycle. This allows for high total pressure recovery and inlet efficiency, as defined below [49]:

$$P_{\text{R, tot}}(M < 1) = \frac{P_\text{f}}{P_\infty} \qquad \eta = \frac{P_\text{f}}{P_\text{i}}$$

$P_\text{i} \equiv$ Intake Pressure $\qquad\qquad$ $P_\text{f} \equiv$ Exhaust Nozzle Pressure
$P_{\text{R, tot}} \equiv$ Total Pressure Recovered $\qquad$ $\eta \equiv$ Efficiency
$P_\infty \equiv$ Free Stream Pressure $\qquad\qquad$ $M \equiv$ Mach Number

For aircraft velocities less than Mach 1, $P_\text{f} \approx P_\text{i}$. Conversely, at velocities greater than Mach 1, the cone extends to decrease the bypass ratio and optimize the lead shock position. This decelerates the intake air speed over the subsequent series of shocks, which reduces the total pressure recovery to the following relation:

$$P_{\text{R,tot}}(M > 1) = \eta[1 - 0.075(M - 1)^{1.35}]$$

It is clear that below Mach 2, corresponding to the N+1 and N+2 NASA Current Technology Goals for Future Supersonic Vehicles, this accounts for a small loss in pressure recovery. The second main propulsion performance reduction is due to spillage drag, which occurs when an inlet spills air around the lip instead of conducting it to the pressure face, as defined below:

$$D_{\text{spill}} = K\big[\dot{m}(V_\text{i} - V_\text{f}) + A(P_\text{i} - P_\infty)\big]$$

where K is the lip suction factor, $\dot{m}$ is the mass flow rate, $V_\text{i} - V_\text{f}$ is the velocity change upon entering the inlet, and A is the inlet's cross sectional area. The relevant point is that the small engine dimensions require a small inlet frontal area, which decreases the spillage drag contribution.

Many design features from the past reappear on Goldeneye's engines to optimize performance. Cowl bleeds redirect incoming air through shock traps to provide subsonic cooling air to the rest of the engine, later drawn out of the nacelle by the fast-moving exhaust flowing through the ejector. For take-off and landing, where $M < 0.5$, multiple ports open along the nacelle to bring air at ambient temperature and pressure to the engine components through valves exposed to heat exchangers [50], which consist of tubular-array and micro-channel plate configurations of coolant-carrying pipes. Recent efforts, most notably Reaction Engine's SABRE engine [51–54], have been able to reliably construct pre-cooler devices[2] composed of thousands of thin-walled, small-diameter tubes, which provide large surface area and low weight, made possible by advances in industrial micrometer construction. The open ports take advantage of the low pressure in the bypass channel to draw air through the tube arrays, which is chilled by small volumes of rapidly cycling coolant, decreasing the temperature of the air that is subsequently used to draw heat from the engine. This optimizes engine

---

[2]The most advanced pre-cooler devices cool intake air for hypersonic aircraft travelling at $M \geq 5$; A similar construction would be much more effective for cooling air of lower temperatures during takeoff and landing.

performance, which is beneficial for a high climbing rate out of a commercial airport with physical limitations[3].

4.4 Exhaust Nozzles

Turbojet engines offer a significant improvement over turbofans at speeds greater than Mach 1.5. They compress the entirety of the intake flow into the core, which is then energized and exhausted at high velocity and temperature to produce pure thrust. The Rolls-Royce/Snecma Olympus 593 engine took advantage of the high-speed cruise benefits of the turbojet, rendering the Concorde's propulsion as efficient as possible under the technical limitations of the time, and echoed later in the Pratt & Whitney F119 and General Electric F120 [33]. With that being said, turbofan engines excel in the high subsonic and low supersonic range, bestowing greater cruise efficiency to the design along with quieter takeoff acceleration[4]. Thus, for an adaptable and commercially practical supersonic business jet like Goldeneye, an engine that acts as both a turbofan and turbojet is optimal.

Debiasi and Papamoschou present a Targeted Mach Wave Elimination (TMWE) bypass design [31] that couples the core exhaust with a variable secondary bypass flow. This shields the mach waves produced by the turbulent eddies during the interaction of the exhaust stream with the environment, accompanied by primary bypass flow with a high bypass ratio (BPR). When the aircraft is in the subsonic and low supersonic segments of flight[5], the bypass gates (labeled A in Figure 13 below) are opened, increasing the BPR to provide greater lift.
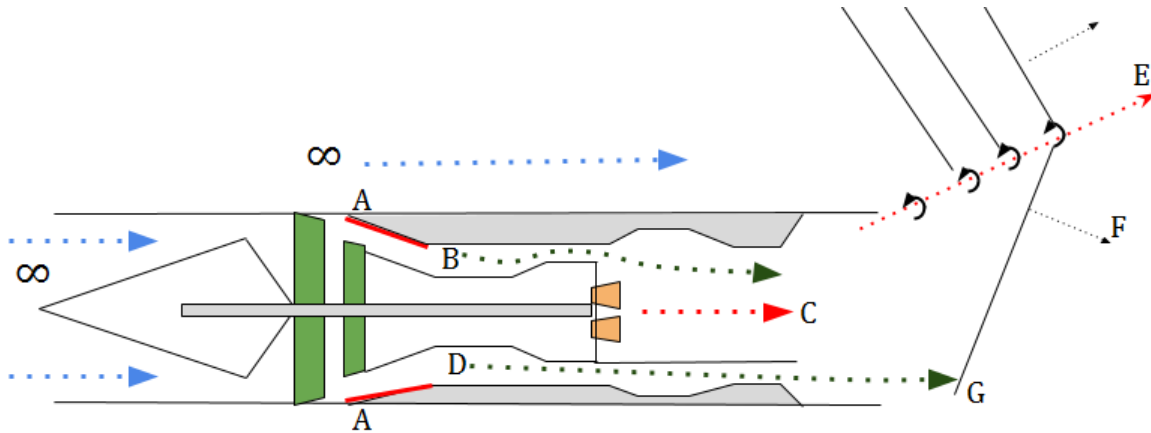

Figure 13: Diagram of the engine when the relative ambient airflow (∞) is at $M \leq 1.5$. A labels the retracted gates, which allow flow to the bypass chambers, B is the primary bypass path, and C is the mixing of the core flow and primary bypass flow. Turbulent eddies travelling along E produce Mach waves along F. The secondary bypass flow at D suppresses the descending Mach waves at G.

---

[3]For example, San Diego International Airport has multiple restrictions due to topographical features that necessitate a steep climb rate, preventing heavier aircraft from landing.
[4]This is achieved by accelerating a larger mass flow at lower speed.
[5]From takeoff ($M = 0$) to transonic acceleration ($M \approx 1.5$).

The intake stream is then separated into core and bypass flow, the latter of which is subdivided further into a primary and secondary stream with a $B{:}D$ ratio of 1.5, so that 40% of the bypass is redirected for targeted noise suppression while 60% is harnessed to increase thrust. $\dot{m}_p$ and $\dot{m}_s$[6] are manipulated by compression and expansion completely independently, allowing the velocity difference ΔU between U_{core} and U_p to be maximized for optimal thrust. However, the ΔU between U_{core} and U_s is moderate, acting as a mediator between the core flow and the ambient flow while simultaneously suppressing the Mach waves created by the mixing of the core and primary bypass streams. This concept is put into practice with a primary nozzle placed where these two flows mix and with a secondary nozzle where the exhausts of the primary nozzle and the secondary bypass flows mix.

Debiasi and Papamoschou also show experimentally that coaxial[7] eccentric[8] nozzles are effective in mitigating downward noise originating from the elongated core of a turbojet engine [34–37]. Below, Figure 14 depicts the secondary flow D exhausting from the secondary nozzle and the shielding in the G region from the noise source region C. Because the secondary stream, whose velocity is closer to that of the surrounding flow, physically interferes with the mach waves, the noise is dampened and redirected such that the noise distribution with respect to arc angle has lower kurtosis[9]. The noise is therefore more evenly dissipated at lower amplitude over a large angular range, replacing the piercing scream of the turbojet with a rumble indistinguishable from other aircraft sporting turbofan engines. This is shown in Fig. 8a of [31] (not displayed). Scale model testing shows a 17% (119 to 98 dB) reduction in noise of peak noise emissions directly behind the aircraft over frequencies greater than 50 Hz, and a 3.03% (99 to 96 dB) to 9.24% (106 to 98 dB) reduction in the lateral direction from 500 to 2000Hz for an A-weighted spectrum[10].

Figure 14: A simplistic diagram of the exhaust nozzles of an engine, as viewed from behind the aircraft. The letters correspond to Figure 13; B is the primary bypass, which mixes with the core flow at C. The geometry here need not be concentric, but must be designed for optimal BRP and thrust performance at subsonic and low-supersonic ambient airspeeds. The secondary bypass flow, D, then mixes with the exhaust of the primary nozzle and is directed downwards since $\delta_v > \delta_h$, suppressing the Mach waves in the G region.
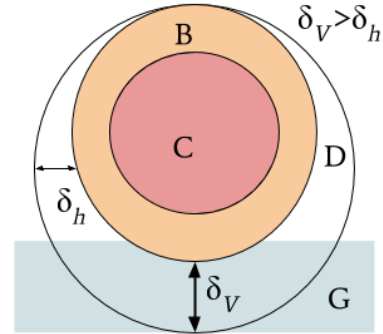
The derivation of the thrust for the TMWE design in [31] follows the Hill & Peterson approach to thermodynamic analysis [38] and non-dimensionalizes the mass flow rates in each engine component[11]. The total thrust of the engine is given by equation 25 of [31]:

$$F_{tot} = F_p + F_s = \dot{m}_p U_p + A_p(p_p - p_\infty) + \dot{m}_s U_s + A_s(p_s - p_\infty) - \dot{m}_\infty U_\infty$$

$p \equiv$ Primary Nozzle Exhaust $\qquad$ $s \equiv$ Secondary Airflow
$F \equiv$ Thrust $\qquad$ $\dot{m} \equiv$ Mass Flow
$A \equiv$ Area $\qquad$ $P \equiv$ Pressure
$\rho \equiv$ Density $\qquad$ $U \equiv$ Velocity

---

[6] $B{:}D = \dot{m}_p{:}\dot{m}_s$, where $\dot{m}_p \equiv$ primary bypass mass flow rate, and $\dot{m}_s \equiv$ secondary bypass mass flow rate.

[7] The primary nozzle is encompassed in the secondary nozzle, and often releases exhaust before the secondary nozzle.

[8] Nozzle design featuring an off-center alignment between the two coaxial nozzles along one axis. In figure 14, the primary nozzle is shifted vertically with respect to the secondary nozzle.

[9] While kurtosis is not a measurement of the flatness, sharpness, or modality of a curve (as it is sometimes misinterpreted to be), the dominant skewer of the noise distribution for a standard turbojet is not present when compared to designs featuring TMWE [31]. This means that the noise is evenly distributed at the tails of the curve, as it is in the center, and implies noise dissipation in all directions [46, 47].

[10] A noise spectrum perceived by the human ear

[11] "To compare results relative to different cycles adopting the same engine core, it is proper to non-dimensionalize the mass flow rates in each engine component with respect to the mass flow rate in the compressor." [31]

17

The surface areas A of the nozzles, considered over a vertical plane, are defined by eqns. 23 and 24 of [31]:

$$A_p = \frac{\dot{m}_p}{\rho_p U_p} = \frac{\dot{m}_{com} m_{r_p}}{\rho_p U_p}$$

$$A_s = \frac{\dot{m}_s}{\rho_s U_s} = \frac{\dot{m}_{com} m_{r_s}}{\rho_s U_s}$$

where com represents the compressor. Pressure is calculated by $P = \rho R T$, where $\rho = \frac{m}{v}$ is the density, R is the gas constant, and T is the temperature at the location of interest. The nozzle exit velocity is defined by equation 22 of [31], $U = M\sqrt{\gamma R T}$, where M is the Mach number and $\gamma = c_p/c_v$ is the specific heat ratio. The corrected compressible mass flow rate is then given by equation 1 of [39]:

$$\dot{m} = \frac{A P_{\text{tot}}}{\sqrt{T_{tot}}} \sqrt{\frac{\gamma}{R}} M \left(1 + \frac{\gamma - 1}{2} M^2\right)^{-\frac{\gamma + 1}{2(\gamma - 1)}}$$

Alternatively, the corrected compressible mass flow rate, equation 2 of [39], can be found by dividing by a factor of $g = 9.81$ m/s^2 and by considering the temperature ratio, $\Theta = \frac{T}{T_\infty}$, and the pressure ratio, $\delta = \frac{P}{P_\infty}$, yielding: $\dot{m} = \frac{\dot{W}\sqrt{\Theta_t}}{g A \delta_t}$, which for air computes to:

$$\dot{m} = \frac{1}{g} 0.59352 M (1 + 0.2 M^2)^{-1} \zeta_{\dot{m}} \frac{\text{kg}}{\text{s } m^2}$$

where $\zeta_{\dot{m}} = 70.3069 \frac{\text{lb}}{\text{s in}^2} \frac{\text{s } m^2}{\text{kg}}$ is the unit conversion factor for mass flow from American to SI units.
To calculate the total thrust capability of each engine, it is assumed that the gas constant of air does not significantly differ in the temperature range of 300-1500 K nor in the pressure range of air in the altitude range of 0-20 km [40–42].

Name	Abbreviation	Valves Open	Valves Closed	Source
Acceleration due to gravity	g	9.81 $\frac{\text{m}}{\text{s}^2}$	-	[d]
Mach number of primary flow velocity (M)	M_p	5	4	[31]
Temperature of primary flow (K)	T_p	1800	1700	[43–45]
Mach number of secondary flow velocity (M)	M_s	0.4	-	[31]
Temperature of secondary flow (K)	T_s	550	N/A	[a]
Ratio of primary to secondary bypass volumes.	$U_p{:}U_s$	10:1	$U_p : 0$	[a]
Ambient air velocity (M)	U_∞	0.4	1.8	[a]
Average specific heat ratio	γ	1.36	-	[31]
Gas constant of air ($\frac{\text{J}}{\text{kg} \cdot \text{K}}$)	R	287	-	[40–42].
Density of air at 0 km elevation ($\frac{\text{kg}}{\text{m}^3}$)	ρ_∞	1.225	-	[40]
Density of air at 20 km elevation ($\frac{\text{kg}}{\text{m}^3}$)	ρ_∞	0.089	-	[40]
Temperature of air at 0 km elevation (K)	T_∞	300.00	-	[a]
Temperature of air at 20 km elevation (K)	T_∞	216.65	-	[41]

[a]≡assumed, [d]≡datum.

Table 1: Parameters used for the thrust, exhaust nozzle area, and mass flow calculations.

Figure 15 below conveys the relationship between the cross sectional areas of the primary and secondary exhaust nozzles. When the bypass valves are open to the secondary bypass (at subsonic, transonic, and low supersonic speeds) the maximum thrust value is increased by a greater secondary bypass, shown by the plot in 16a. However, the thrust relation plot in 16b demands a large primary nozzle area. Optimizing the surface area of the primary and secondary exhaust nozzles results in a ratio of $\frac{A_p}{A_s} \approx 1.4 = \frac{3.5}{2.5}$. As discussed in Section 4.1, the total diameter of each engine must be 0.684 m, implying that the combined nozzle area must be 1.469 m^2 for a circular cross section. Therefore, the cross sectional areas are 0.857 m^2 for the primary exhaust nozzle and 0.612 m^2 for the secondary nozzle. The secondary nozzle does not require significant modification of current exit nozzle designs, and its modest area requirement allows it to fit tidily underneath the primary nozzle, eliminating any significant deviations from well-tested exit nozzle designs.
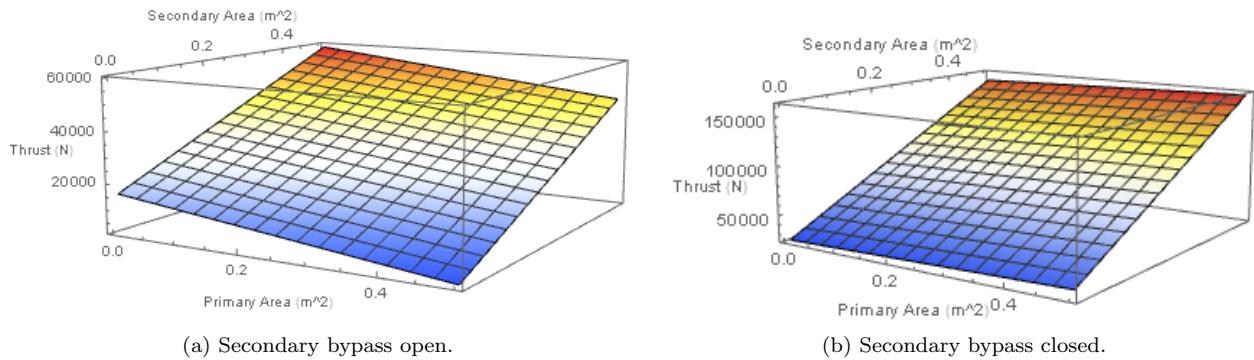

(a) Secondary bypass open.   (b) Secondary bypass closed.

Figure 15: Thrust in Newtons as a function of primary exhaust nozzle area and secondary bypass area. Note that since $\dot{m} \propto \frac{1}{\text{BPR}}$, the optimization lies in the ratios that will give a maximum thrust when the bypass valves are (a) opened for increased lift at $M \leq 1.5$, and (b) closed for supersonic cruise (BPR $= 0$).

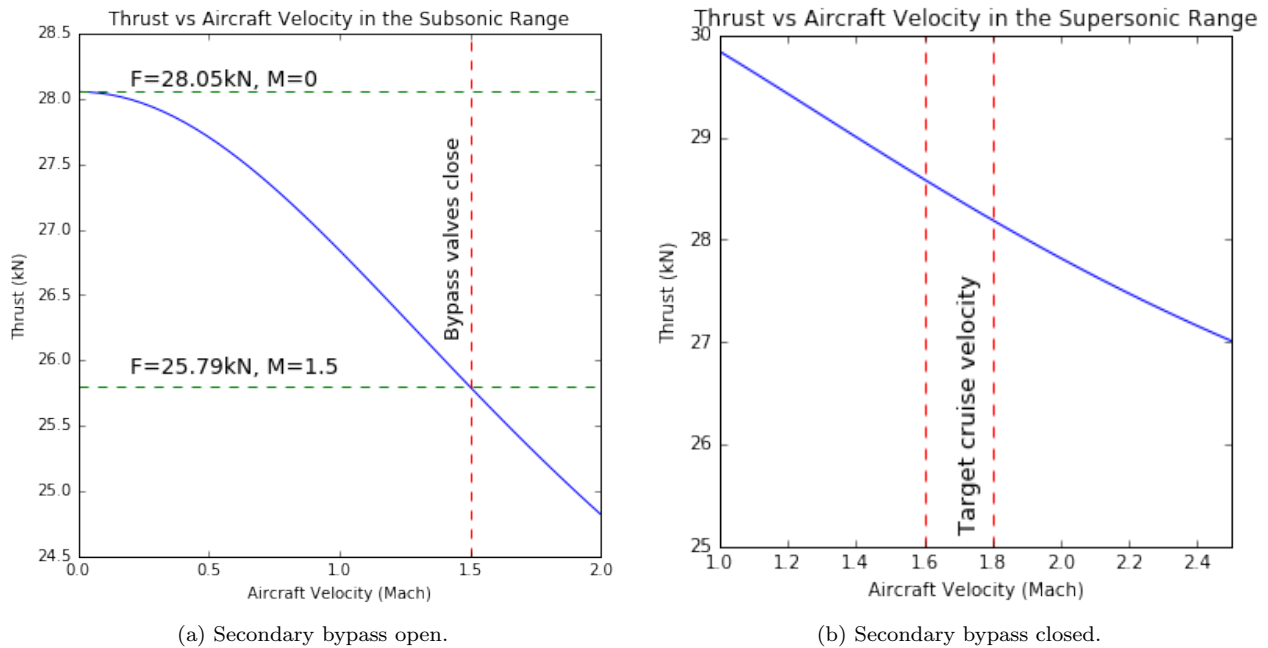(a) Secondary bypass open.   (b) Secondary bypass closed.

Figure 16: Thrust in Newtons as a function of aircraft velocity for a single engine. At all velocities, the thrust exceeds the cruise requirements and is capable of a thrust increase of 255% for take-off and landing. To calculate the total thrust, both engines must be accounted for.

For the TMWE, velocity is inversely related to the thrust whether or not the secondary nozzle is active, as visible in Figure 16 above. The values are independently calculated for the two engines, so thrust is assumed to combine linearly. In both velocity ranges, the maximum thrust of each engine exceeds the previously calculated cruise thrust of 10.861 kN by a large margin. At takeoff, a 28.053 kN thrust yields a 17.192 thrust kN margin to increase lift, allowing for a shorter runway and making it feasible for Goldeneye to access airports used by small business jets. Less thrust during takeoff and landing reduces noise emissions, easing permission-of-use discussions with authoritative bodies from communities near airports (city and state governments, noise pollution committees, etc.).

Increased thrust is required in the transonic region, which must be traversed quickly to avoid high fuel costs associated with the spike in drag. A thrust of 27.227 kN at $M_\infty = 0.8$ and a thrust of 26.840 kN at $M_\infty = 1.0$ give a margin of roughly 16 kN per engine in the transonic range. At cruise velocities of Mach 1.6-1.8, the thrust ranges from 25.191 kN to 25.589 kN, giving 14.728 kN to 14.330 kN of additional available thrust. While this is less than when the secondary bypass is active, there is also less need for additional thrust, excluding emergencies. At all velocities, it is possible to sustain the cruise thrust with some additional thrust remaining. In the case of an engine failure during supersonic cruise, the second engine can sustain stable supersonic flight until the aircraft is safely decelerated below the supersonic range. The increased thrust at subsonic speeds allows for a longer travel range, allowing the aircraft to safely reach airports in the event of an emergency while over the ocean.

4.5   Materials

The engine intake fan must withstand all weather conditions and foreign object ingestion. Because the engines are mounted on top of the fuselage, there is reduced risk from debris on taxiways and runways, but the possibility of bird strike is still a concern. During operation, fan blades are subject to intense tensile stress and therefore must be strong and corrosion-resistant, as well as light to minimize the fan's moment of inertia. However, relative to other engine components, the intake fan does not experience extremely high temperatures, and does not carry as strict of a temperature requirement. Precipitation-hardened 6061 aluminum provides the necessary creep and corrosion resistance, while having an excellent strength-to-weight ratio.

On the other hand, the turbine fan imposes a vastly different set of design challenges. Temperatures inside the turbine may reach excesses of 1000 °C, and the tremendous angular velocity of the fan imposes extreme tensile loads on the blades. In this environment, deformation from creep, a temperature-dependent process, becomes a major issue. Traditionally, turbines have been fabricated from nickel-based superalloys such as Nimonic and Inconel. Inconel 792 is precipitation-strengthened and very resistant to creep and corrosion at high temperatures, making it an attractive option for the turbine fan blades.

Another approach to combating creep is to enlarge the grain boundaries in the material, minimizing the net diffusion of atoms along them, which is responsible for localized slipping. Turbine blades can be manufactured from a single crystal, so that they effectively contain no grain boundaries. This removes the possibility of Coble creep and eliminates the risk of weakened grain boundaries by corrosion. Single crystals of superalloys such as CMSX-6 have been harvested to make turbine fan blades, making them another smart choice for this component [30].

The combustion chamber operates under similar conditions to the turbine, but at even greater temperatures. Because there is no stress from rapidly moving parts, high-temperature alloys that are corrosion-resistant even at high temperatures, such as Ti-5553, are suitable. Ti-5553 is easily castable, facilitating the ease of manufacturing of the complex geometries in combustion chambers. Furthermore, temperatures within the combustion chamber can be controlled by careful planning of air cooling techniques. Finally, coatings derived from zirconium dioxide or yttrium oxide provide thermal insulation at the surface without sacrificing the ductility of the alloy.

5 Design Implementation

5.1 Wing Size

The wing's geometry was parameterized in Section 2.3 with the outline of a planform wing shape based on the root chord-length (R), the leading edge's sweep angle (Λ), and the trailing edge's sweep angle (Λ_{rear}). To produce a final wing shape and size, these parameters must be varied to create the optimal conditions for both supersonic cruise and subsonic flight. As previously discussed, the optimal leading and trailing sweep angles are set to $\Lambda = 60°\, and \,\Lambda_{\text{rear}} = 60°$. A decrease in the leading angle results in a higher aspect ratio and provides more lift at the expense of the leading edge crossing paths with oblique shock waves. An increase of the trailing angle also increases the clipped delta wing surface area for lift during supersonic flight, but decreases the size of the radial extension, thus diminishing subsonic flight performance. After conducting 25 flow simulations at both supersonic cruise and standard temperature and pressure (STP) conditions, it was discovered that compromises to either of the angles are not necessary to enable highly efficient supersonic flight.

The behaviour of laminar airfoils is analogous to that of the centerboard or keel of a sailboat; the flow around them is streamlined and relatively symmetrical, especially in comparison to a conventional airfoil. As such it will not provide much lift when its angle of attack is set to zero. However, if rotated even very slightly, the airfoil strongly counters this force. To study this behaviour, prototypes with root chord lengths varying from 8 to 20 meters can be subjected to Mach 1.7 airflow at small incidence angles ranging from 0 to 3 degrees in the flow simulator. To validate this approach, a replica CAD of the Concorde's wing is built and run under the same simulations. When the results are compared to known Concorde specifications, the model's numerical findings do not correlate perfectly with validated data, but they do follow the expected general trends previously discussed.

This paper only outlines a conceptual design of Goldeneye AB1, so certain approximations must be made in order to use the fully loaded aircraft mass figure. The Gulfstream G280 is chosen as a reference aircraft for this purpose. Its maximum load mass is 17962.2 kg, corresponding to a weight of 176030 N. As the G280 is designed to carry 20 passengers—8 more than the AB1—over similar ranges to Goldeneye, an absolute upper bound of the AB1's load capacity is taken to be approximately 75% of the Gulfstream's weight, a figure that accounts for AB1's smaller size, lighter materials, and larger fuel capacity. The lift is found in general to increase exponentially as a function of incidence angle, and approximately linearly for small incidence angles. Testing various wing sizes at flow incidence angles between $0.5°$ and $1.7°$, enough lift is generated to reliably carry AB1's upper mass bound.

Considering that the Concorde's wing simulation produces lift specifications lower than its actual values, the AB1 simulation results strongly validate its wing design, since the actual pitch angle of the aircraft will be lower than the tested values. The root chord length is found to maximize lift efficiency at $R = 15$m, which gives the AB1 a similar planform area to the Aerion supersonic business jet (SBJ), with the added benefit of higher lift at subsonic speeds due to the variable wing geometry. The minimum drag on Goldeneye at Mach 1.7 was calculated at roughly 3000N. At STP, with a pitch angle of $10°$ and takeoff velocity of 300 km/h, the radial extension increases the total lift generated by the wing by about 45%!. This can be attributed to the increase in planform area and to the lower absolute curvature of the wing, since the main chord lengthens, making Goldeneye more resistant to flow separation at large incidence angles. As envisioned, the variable wing geometry of the AB1 shows great promise.

5.2 Canard, Vertical Stabilizer, and Engine Mount

The AB1's canard takes after the Eurofighter Typhoon's, a foreplane with approximately one third of the wing's area that features a full-span slotted elevator for pitch control. The canard is placed on the nose just in front of the cockpit to form a closely coupled configuration, lying ahead and slightly above the wings. A canard mounted in this manner provides a greater pitching moment for a given angle of attack (See Figure 17 on the following page), which is desirable since the foreplane is the prime control surface for the aircraft's pitch. Furthermore, the close-coupled configuration provides additional lift during takeoff, landing, and supersonic

cruise [28]. Not only does the upraised canard mount inhibit destabilization of airflow over the wing at supersonic speeds, it actually makes the flow more stable at subsonic speeds by redirecting it downwards over the wing, which at high angles of attack induces a wake vortex above the wing that generates vortex lift [29].
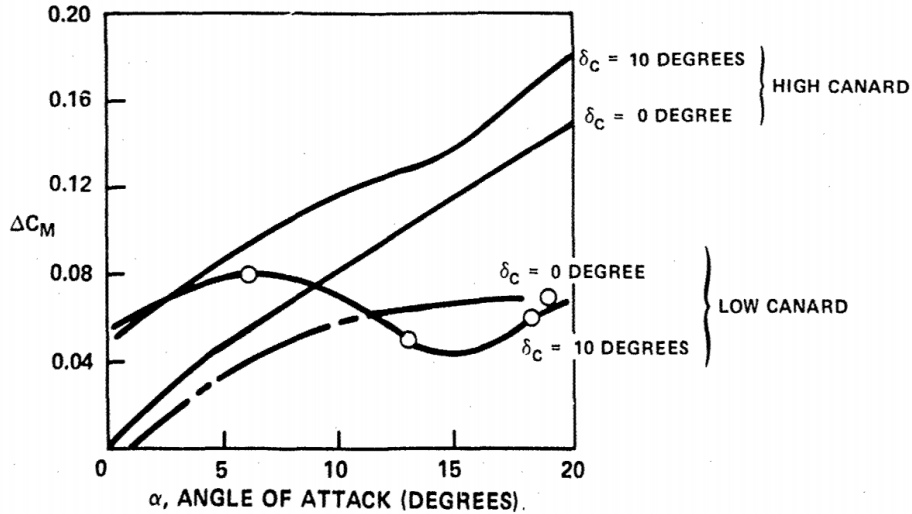

Figure 17: Pitching moment coefficient with respect to angle of attack for high and low-mounted canards at different pitch angles. The pitching moment increases more drastically with angle of attack in the high mount configuration, vastly outperforming the low mount and making it virtually impossible to stall.

The canard planform is a truncated, 45° clipped delta shape, selected for its high lift coefficient and lift-to-drag ratio [55]. The AB1's canard features the same NACA 66-206 airfoil as the wings because this profile satisfies the desired laminar flow separation in the supersonic region.

A vertical stabilizer is placed between the engine casings on top of the fuselage to provide yaw stability and control, although this is less of a concern than the horizontal stability. The stabilizer's airfoil is the NACA 64-008A Airfoil, a symmetrical and highly laminar airfoil with a thickness ratio of 8% that maintains low drag and laminar flow.

Goldeneye's engines are mounted on top of the fuselage toward the rear of the aircraft. As previously discussed, this reduces the noise from the engines that reaches the ground, using the wings as a sound barrier without subjecting them to high thermal stresses. The engines are encased by a nacelle that is blended into the top surface of the wing and is partitioned into two sections to optimize air intake for both engines.

For a conceptual rendition of Goldeneye AB1 that showcases all of these features, see Figure **??** at the end of the paper.

6 Performance Criteria

All required technical design goals are met by the Goldeneye AB1. Because it is very hard to find theoretical values for many of the parameters required to calculate the performance criteria, the best approach to proving this is to use experimental data from existing aircraft with designs inferior to Goldeneye's to find worst case estimates for its specifications. Though it is impossible to prove beyond doubt that the AB1 performs better than its counterparts without real life testing and experimentation, the entire preceding portion of this paper has laid out very convincing arguments with simulated data and careful analysis, pointing to the legitimacy of this claim.

To find an upper bound for the thrust specific fuel consumption ($TSFC$) of its engines, the Concorde's efficiency at supersonic cruise should be appropriately scaled. The efficiency of its Olympus engines varies linearly with velocity [22], and at Mach 2.2, they boast an $TSFC$ of 1.195. Goldeneye's average supersonic cruise velocity of Mach 1.7 is 22.7% lower than the Concorde's, so scaling the $TSFC$ value by the same amount Goldeneye's $TSFC$ is calculated to be 0.923. While this value is lower than most subsonic business jets, note that it is nearly impossible to achieve comparable $TSFC$ values as a supersonic aircraft, and that this estimate is merely a baseline efficiency that does not even account for the performance improvements of the variable geometry inlet.

Given this value, a lower bound for Goldeneye's range can be estimated by the Bregeut Range Equation [25]:

$$\text{Range} = \frac{v \cdot \frac{C_L}{C_D}}{g \cdot TSFC} \cdot \ln\left(\frac{W_{\text{initial}}}{W_{\text{final}}}\right)$$

where v is the plane's velocity, g is the acceleration due to gravity, W_{initial} is the initial weight of the aircraft, and W_{final} is its final weight. A $W_{\text{initial}}/W_{\text{final}}$ value of 1.5 implies that Goldeneye carries half as much of its dry weight in fuel, a reasonable that is true of many business jets currently in service, including the Gulfstream G280 [24], previously used for a mass estimate of the AB1. In fact, because it is a supersonic airliner, if anything Goldeneye would probably have a higher actual $W_{\text{initial}}/W_{\text{final}}$ than subsonic business jets, which would increase its range. In any case, a lower bound for Goldeneye's range is calculated to be 4227 nautical miles.

Obviously, the AB1 meets the cruise speed target of Mach 1.6–1.8 and the payload of 12 passenger since it was designed from the ground up to meet these parameters. With a TSFC of 0.923 and engines capable of supplying 4883.29 lbf (21722N) of thrust, Goldeneye can cover its maximum range in just 3.96 hours at Mach 1.6 (1066.78 knots). This flight requires 17853 pounds of fuel, so Goldeneye's fuel efficiency comes out to 2.84 passenger-miles per pound of fuel, far exceeding the design requirement of 1.00 at cruise conditions. Under those circumstances, the AB1 consumes merely 35.2% of the amount of fuel that could be consumed while still meeting the fuel efficiency goal.

For the sake of calculation, Goldeneye's takeoff field length can be divided into two segments: takeoff ground roll and horizontal range required to climb to an altitude of 35 feet, satisfying the Federal Aviation Administration's takeoff minimum. The former is defined as follows:

$$d_{TO} = \frac{m_{TO} \cdot (v_{LO} - v_W)^2}{2 \cdot (F_{TO} - D_{TO} - \mu \cdot (m_{TO} \cdot g - L_{TO}) - m_{TO} \cdot g \cdot \sin\gamma)}$$

$d \equiv$ Distance	$v \equiv$ Velocity = 155kts	$m \equiv$ Mass = 17962kg
$F \equiv$ Thrust = 40000N (Cruise + 18278N)	$D \equiv$ Drag = 29410kN	$\mu \equiv$ Coefficient of Friction = 0.71
$L \equiv$ Lift = 480kN	$\gamma \equiv$ Runway Slope = 0°	Subscript $TO \equiv$ Takeoff
$v_W =$ Wind Speed		

As a preliminary calculation, the runway is taken to be perfectly flat and the wind to be 0 knots, which yields a takeoff ground roll of 1138.07 meters, or 3373.83 feet. To use the remaining 3626.17ft of runway left to clear the takeoff screen, Goldeneye must climb at an minimum angle of 0.55°. A climb angle of 10° comfortably clears the end of the runway by a vertical distance of 639.39 feet, and a maximum climb angle of 15° gives 971.63 feet of vertical clearance.

7   Conclusion

The feasibility of developing Goldeneye comes down to design challenges, developmental roadblocks, and economics. Goldeneye's propulsion is an offshoot of a tried and true engine. Many of the most daunting engineering challenges with which engine production would normally be faced have already been addressed by decades of research and development leading up to the Concorde's release. Goldeneye need only incorporate existing technology to build its propulsion system, which directly reduces R & D costs. More importantly, these improvements bolster the AB1's fuel efficiency, which would reduce prices and make the plane more commercially viable. This is especially important considering that business jets are normally a luxury that most people cannot afford, marketed exclusively to the wealthy. By making high-end supersonic air travel my affordable, Goldeneye could reach more customers than its competitors and tap further into the market, which would increase competition and improve the industry as a whole. If eye-catching enough, the modification of the Olympus 610 engine could hopefully be undertaken in conjunction with Rolls-Royce, the engine's original manufacturer, whose collaboration would significantly aid Goldeneye's team both financially and scientifically by providing funding, support, and a swath of knowledge about the engine it spent so long developing.

The most significant implementation challenge of the AB1 is its retractable wing panel. The wing's hollow internal structure is heavily loaded by the panel and its tracks, which may be subject to jams and actuation malfunction. To address this issue, regular inspection and maintenance of the mechanism above and beyond the already stringent regulations and safety requirements to which aircraft are held would be essential to minimize the risk of mechanical failure. From a material cost standpoint, the use of components such as titanium spars and fasteners may drive up fabrication costs. However, recent manufacturing advancements may facilitate ease of production for some required components. Selective Laser Sintering (SLS) could be used to rapidly prototype and test the system. This process consists of scanning a laser over metal particles at specific points in space to form the desired three-dimensional part, enabling swift integration and cost reduction [?].

With this in mind, Goldeneye would seek to take advantage of existing aerospace alloys and other commonly used materials. Consequently, its manufacturing facilities would not require extensive modification or retooling outside of some very specific modern manufacturing processes necessary for the production of complex parts. Many of the metals most heavily used in Goldeneye's design are readily available and relatively cheap. The fuselage's Ti-6Al-4V alloy is used extensively outside of the aerospace industry in chemical and biomechanical applications. Its ubiquity serves to reduce costs at every stage of production from bulk material purchasing to manufacturing. Similarly, 7075 aluminum, found in the wing spars and ribs, and 6061 aluminum, found in the engine intake fan and other internal elements, have long, distinguished histories of involvement in aircraft construction. Their relatively low cost and high reliability make them very well suited for Goldeneye's production. Inconel 792, used in the turbine fan, is a sand-castable alloy, produced by a method that allows for the fabrication of complex part geometries in a much more affordable manner than comparable processes. Ti-5553, present in the engine combustion chamber, is also easily castable. By purchasing common, high-quality materials in bulk and taking advantage of efficient and advanced manufacturing processes, the price to build and fly the AB1 would be significantly reduced.

Goldeneye's greatest strength would perhaps lie in its innovative features and marketable appeal. People will always want a part of the latest technology, regardless of the industry. This is readily obvious by observing how so many companies try to market and sell their products, from iPhones to Teslas and everything in between. Goldeneye is by definition already on the cutting edge of the aerospace industry simply by being bold enough to spearhead the effort to reintroduce commercial supersonic aviation to the world. But more than that, the AB1's technological innovations could make it relevant for decades to come. True variable wing geometry has never before been attempted by a commercial plane, and certainly not in the way Goldeneye's radial mechanism works. On top of being exciting , sexy, and highly advertisable, this keystone of the AB1 design could genuinely have the ability to revolutionize not just commercial air travel, but the aerospace industry as a whole, from private companies to the armed forces. This combination of practicality, versatility, and allure is what ensures Goldeneye's prolonged success.

Figure 18: Conceptual rendition of the Goldeneye AB1 supersonic business jet in supersonic cruise wing configuration, with its canard, vertical stabilizer, and engine nacelles on display.

Acknowledgements

References

[1] Kumar, M., Kannan, M., Kumar, V., Manigandan, A., Praveen, G. "Analysis of Shock over NACA 66-206 at Supersonic Regime". Advances in Aerospace Science and Applications, Vol. 3, No. 2, pp. 125-130, Hindustan University, Padur, India, 2013.
https://www.ripublication.com/aasa/aasav3n2spl_16.pdf

[2] Wang, F., Milanovic, I., Zaman, K., Povinelli, L. "A Quantitative Comparison of Delta Wing Vortices in the Near-Wake For Incompressible and Supersonic Free Streams". J. Fluids Eng 127(6), 1071-1084, July 12, 2005.
http://fluidsengineering.asmedigitalcollection.asme.org/article.aspx?articleid=1430232

[3] Kroo,I: "Unconventional Configurations for Efficient Supersonic Flight." Stanford University June 6, 2005. Page 13.
http://aero.stanford.edu/reports/vki_kroo_supersonics.pdf

[4] Sadraey, Mohammad: "Aircraft Design: A Systems Engineering Approach." Chapter 5. Wiley, 2012. Page 176.
http://www.academia.edu/4573651/Wing_Design_i_Chapter_5_Wing_Design_Mohammad_Sadraey

[5] Sadraey, Mohammad: "Aircraft Design: A Systems Engineering Approach." Chapter 5. Wiley, 2012. Page 235,239.
http://www.academia.edu/4573651/Wing_Design_i_Chapter_5_Wing_Design_Mohammad_Sadraey

[6] Sadraey, Mohammad: "Aircraft Design: A Systems Engineering Approach." Chapter 5. Wiley, 2012. Page 205
http://www.academia.edu/4573651/Wing_Design_i_Chapter_5_Wing_Design_Mohammad_Sadraey

[7] Sadraey, Mohammad: "Aircraft Design: A Systems Engineering Approach." Chapter 5. Wiley, 2012. Page 224
http://www.academia.edu/4573651/Wing_Design_i_Chapter_5_Wing_Design_Mohammad_Sadraey

[8] Mason, W.H.: "Supersonic Aerodynamics." Virginia Tech. 7/31/2016. Chapter 10, page 20.
http://www.dept.aoe.vt.edu/ mason/Mason_f/ConfigAeroSupersonicNotes.pdf

[9] Mohan Kumar G, Manoj Kannan G, Vignesh Kumar R, Manigandan A, and Praveen G: "Analysis of Shock over NACA 66-206 at Supersonic Regime." Advances in Aerospace Science and Applications. ISSN 2277-3223 Volume 3, Number 2 (2013), pp. 125-130
https://www.ripublication.com/aasa/aasav3n2spl_16.pdf

[10] Jones, Robert T: "Report 1284: Theory of Wing-Body drag at Supersonic Speeds." NACA Cranfield, United Kingdom. 1956.
http://naca.central.cranfield.ac.uk/reports/1956/naca-report-1284.pdf

[11] Sadraey, Mohammad: "Aircraft Design: A Systems Engineering Approach." Chapter 5. Wiley, 2012. Page 223.
http://www.academia.edu/4573651/Wing_Design_i_Chapter_5_Wing_Design_Mohammad_Sadraey

[12] ConcordeSST.com: "Concorde Technical Specs: Fuel system."
http://www.concordesst.com/fuelsys.html

[13] Hall, Nancy: "Center of Pressure." NASA, Glenn Research Center.
https://www.grc.nasa.gov/WWW/k-12/airplane/cp.html

[14] Cornei, Simona: "Mach number, relative thickness, sweep and lift coefficient of the wing - An empirical investigation of parameters and equations." Department of Automotive and Aeronautical Engineering, Hamburg University of Applied Sciences. 31/05/2005.
http://www.fzt.haw-hamburg.de/pers/Scholz/arbeiten/TextCiornei.pdf

[15] NACA 66-206
http://airfoiltools.com/airfoil/details?airfoil=naca66206-il

[16] Araujo, G., Almeida, S."Design Procedure for a Fowler Flap Mechanism". 18th International Congress of Mechanical Engineering, Ouro Preto, Brazil, November 2005.
http://www.abcm.org.br/anais/cobem/2005/PDF/COBEM2005-0040.pdf

[17] Grumman F-14 Tomcat
https://en.wikipedia.org/wiki/Grumman_F-14_Tomcat#Variable-geometry_wings_and_aerodynamic_design

[18] Concorde Elevons and Rudders
http://www.heritageconcorde.com/concorde-elevons-and-rudder

[19] Interference Drag of Wing Mounts
Sadraey, M. H., Wing Design, in "Aircraft Design: A Systems Engineering Approach", John Wiley & Sons, Ltd., Chichester, UK, 2012, pp. 12

[20] Sears-Haack Body
Ashley, H., Landahl, M., "Aerodynamics of Wings and Bodies", Addison-Wesley, 1965.

[21] Airplane Aerodynamics and Performance, Roskam Jan and Lan C E

[22] Propulsion and Efficiency, SMU Lyle School of Engineering
http://lyle.smu.edu/propulsion/Pages/efficiency.htm

[23] Aircraft Performance, MIT OCW
ocw.mit.edu/ans7870/16/16.unified/propulsionS04/UnifiedPropulsion4/UnifiedPropulsion4.htm

[24] Gulfstream G280 Specifications
gulfstream.com/aircraft/gulfstream-g280

[25] Bregeut Range Notes, Fall 2008, MIT
web.mit.edu/16.unified/www/FALL/Unified_Concepts/Breguet-Range-U2-notes-Fall08(2).pdf

[26] Saturn V Launch Simulations
braeunig.us/apollo/saturnV.htm

[27] Aspects of Aircraft Design and Control, Olivier Cleynen, May 2014
documents.ariadacapo.net/cours/aspects_aircraft_design/lecture_8.pdf

[28] Anderson, Seth B. "A Look at Handling Qualities of Canard Configurations". NASA, September 1986.
https://ntrs.nasa.gov/archive/nasa/casi.ntrs.nasa.gov/19870013196.pdf

[29] "Jet Aircraft – Effect of a close-coupled canard on a swept wing". SAI Research Report (Abstract). Sage Action, 2009.
http://www.sageaction.com/aircraft_testing1.htm#JetAircraft

[30] Onyszko, A., and Kubiak K., "Method for Production of Single Crystal Superalloys Turbine Blades", *Archives of Metallurgy and Materials*, Vol. 54, No. 3, 2009, pp. 765-771.

[31] Debiasi, M., and Papamonschou, D. "Cycle Analysis for Queiter Supersonic Turbofan Engines", University of California, Irvine, 2001.

[32] Papamoschou, D., and Debiasi, M., "Directional Suppression of Noise from a High-Speed Jet", *AIAA Journal*, Vol. 39, No. 3, 2001, pp. 380-387.

[33] Sweetman, B., "YF-22 and YF-23 Advanced Tactical Fighters", Motorbooks International, 1991, Osceola, WI, pp. 61-64.

[34] Murakami, E., and Papamoschou, D., "Mixing Layer Characteristics of Coaxial Supersonic Jets", *AIAA Journal*, 2000-2060.

[35] Papamoschou, D., "Mach Wave Elimination from Supersonic Jets" *AIAA Journal*, Vol.35, No.10, 1997, pp.1604-1611

[36] Papamoschou, D., and Debiasi, M., "Noise Measurements in Supersonic Jets Treated with the Mach Wave Elimination Method",*AIAA Journal*, Vol. 37, No. 2, 1999, pp. 154-160.

[37] Debiasi, M., and Papamoschou, D., "Noise from Imperfectly Expanded Supersonic Coaxial Jets", *AIAA Journal*, Vol.39, No.3, 2001, pp.388-395.

[38] Hill, P., and Peterson, C., "Mechanics and Thermo dynamics of Propulsion", 2nd Ed., Addison Wesley, 1992, New York

[39] Space Flight Systems, Glenn Research Center, Online Educational Material: Corrected Airflow per Area

[40] Cengel, Yunus A., and Boles, Michael A. Thermodynamics: An Engineering Approach. New York, NY: McGraw-Hill, 2011. Print.

[41] Sontag, Borgnakke and Van Wylen. Fundamentals of Thermodynamics. 6th Ed., John Wiley & Sons, Inc., 2003. Print.

[42] Kittel, C., and Kroemer, H. Thermal Physics. 2nd Ed., W.H. Freeman, 1980. Print.

[43] Jackson, P.A. "Jane's all the World Aircraft, 1998-1999", Sentinel House, 1998, Couldson UK.

[44] Roth, B., and Mavris, D., "Analysis of Advanced Technology Impact on HSCT Engine Cycle", AIAA Pap er No. 99-2379, 1999.

[45] Sanghi, V., and Lakshmanan, B.K., "Some Trends in Engine Cycle Selection and Overall Aircraft Sizing", Proceedings of the XIV International Symposium on Air Breathing Engines, ISABE pap er 99-7112, 1999.

[46] Freedman, D., Pisani, R., and Purves, R. "Statistics". 4th Ed., W.W. Norton & Company, 2007.

[47] Devore, J. L. "Probability and Statistics for Engineering and the Sciences". 8th Ed., Cengage Learning, 2011.

[48] American Environment Company, Inc. "Acoustic Power and Sound Pressure Levels of Typical Noise Sources". Medford, N.Y., 2017.

[49] "Inlet Performance", NASA Glenn Research Center, edited by Nancy Hall, 2015.

[50] Webber, H., Feast, S. and Bond, A. "Heat Exchanger Design in Combined Cycle Engines" IAC-08-C4.5.1, 2008.

[51] Mehta, U., Aftosmis, M., Bowles, J., & Pandya, S. "Skylon Aerodynamics and SABRE Plumes". 20th AIAA International Space Planes and Hypersonic Systems and Technologies Conference., Glasgow, Scotland, 2015

[52] Musielak, D. "SABRE: A high speed air breathing rocket engine fo the SSTO SKYLON spaceplane". 2012.

[53] Varvill, R. and Bond, A. "The Skylon Spaceplane: Progress to Realization". JBIS, Vol. 61, pp. 412-418, 2008.

[54] Aggarwal, R., Lakhara, K., Sharma, P.B., Darang, T., Jain, N., Gangly, S. "SABRE Engine: Single Stage to Orbit Rocket Engine".

[55] Lacey, D,. "Aerodynamic Characteristics of the Close-Coupled Canard as Applied to Low-to-Moderate Swept Wings". Vol.1, David W. Taylor Naval Ship Research and Development Center, Bethesda, MD, 1979.
http://www.dtic.mil/dtic/tr/fulltext/u2/a063819.pdf

[56] Rolls-Royce Is Ready For A Supersonic Business Jet
https://airinsight.com/2017/04/10/rolls-royce-ready-supersonic-business-jet/

[57] Liebhardt, B., Lütjens, K. "An Analysis Of The Market Environment For Supersonic Business Jets".
German Aerospace Center-Air Transportation Systems. Hamburg, Germany, 2011.
http://elib.dlr.de/75275/1/DLRK2011_Liebhardt-L%C3%BCtjens.pdf

[58] Supersonic Business Jet Market Expected To Grow 4% Annually
http://aviationweek.com/awin-only/supersonic-business-jet-market-expected-grow-4-annually

[59] Shama Rao, N., Simha, T. G. A., Rao, K. P., Ravi Kumar, G. V. V. "Carbon Composites Are Becoming
Competitive and Cost Effective". Infosys.